International Journal of Pharmaceutics 628 (2022) 122281

Contents lists available at ScienceDirect

International Journal of Pharmaceutics

journal homepage: www.elsevier.com/locate/ijpharm

Pluronic®/casein micelles for ophthalmic delivery of resveratrol: *In vitro*, *ex vivo*, and *in vivo* tests

Maria Vivero-Lopez [a], Chiara Sparacino [a], Ana Quelle-Regaldie [b], Laura Sánchez [b,c], Eva Candal [d], Antón Barreiro-Iglesias [d], Fernando Huete-Toral [e], Gonzalo Carracedo [e], Ana Otero [f], Angel Concheiro [a], Carmen Alvarez-Lorenzo [a,*]

[a] Departamento de Farmacología, Farmacia y Tecnología Farmacéutica, I+D Farma (GI-1645), Facultad de Farmacia, Instituto de Materiales (iMATUS) and Health Research Institute of Santiago de Compostela (IDIS), Universidade de Santiago de Compostela, 15782 Santiago de Compostela, Spain
[b] Departamento de Zooloxía, Xenética y Antropoloxía Física, Facultade de Veterinaria, Universidade de Santiago de Compostela, 27002 Lugo, Spain
[c] Preclinical Animal Models Group, Health Research Institute of Santiago de Compostela (IDIS), 15706 Santiago de Compostela, Spain
[d] Department of Functional Biology, CIBUS, Faculty of Biology, Universidade de Santiago de Compostela, 15782 Santiago de Compostela, Spain
[e] Ocupharm Research Group, Faculty of Optics and Optometry, University Complutense of Madrid, C/Arcos del Jalon 118, 28037 Madrid, Spain
[f] Departamento de Microbiología y Parasitología, Facultad de Biología, Edificio CIBUS, Universidade de Santiago de Compostela, 15782 Santiago de Compostela, Spain

ARTICLE INFO

Keywords:
Mixed micelles
Resveratrol
Pluronic® F127
Zebrafish
In vivo tear fluid levels
Ocular biodistribution

ABSTRACT

Ocular health may strongly benefit from the supply of antioxidant agents that counteract free radicals and reactive oxygen species responsible for long-term eye diseases. Additionally, natural antioxidants like resveratrol can inhibit bacteria growth and restore natural microbiota. However, their use is hindered by limited solubility, fast degradation, and low ocular permeability. This work aimed to overcome these limitations by preparing single and mixed micelles of Pluronic® F127 and casein that serve as resveratrol nanocarriers. Single and mixed (0.1 % casein) micelles (0.0 to −17.0 mV; 2.4 to 32.7 nm) increased 50-fold resveratrol solubility, remained stable for one month at 4 °C, withstood fast dilution, underwent sol-to-gel transitions in the 23.9–27.1 °C range, and exhibited potent antioxidant properties. All formulations successfully passed the HET-CAM assay but showed Pluronic®-casein dose-dependent toxicity in the zebrafish embryo model. Resveratrol-loaded single and mixed micelles (10–15 mM Pluronic® F127) displayed antimicrobial activity against *S. aureus* and *P. aeruginosa*. The micelles favored resveratrol accumulation in cornea and sclera, but mixed micelles showed larger lag times and provided lower amount of resveratrol permeated through sclera. *In vivo* (rabbit) tests confirmed the safety of resveratrol-loaded single micelles and their capability to supply resveratrol to anterior and posterior eye segments.

1. Introduction

The eye is susceptible to oxidative damage and inflammation due to its high metabolic activity and intense exposure to radiations, atmospheric oxygen and pollutants. The most susceptible structures are the lens and, especially, the retina because of its high proportion of lipids, high exposure to visible light, and high oxygen consumption needed to provide the elevated amount of energy demanded (Ung et al., 2017; Behl et al., 2016; Calderon et al., 2017; Dammak et al., 2021).

Reactive oxygen species (ROS) are produced mainly by the mitochondrial respiratory chain, but also in numerous enzymatic and oxidation reactions due to a partial reduction of molecular oxygen (Dogru et al., 2018; Nita and Grzybowski, 2016). The exposition to ROS causes cell injures through oxidative damage of DNA, oxidative modification of proteins and lipid peroxidation of membranes. When a decrease in antioxidant defenses (either enzymatic or non-enzymatic) occurs, the imbalance between antioxidants and pro-oxidants triggers the generation of proinflammatory cytokines and proteolytic enzymes and activates pro-angiogenic routes (Cejka and Cejkova, 2015; Pinazo-Duran et al., 2018). Oxidative stress and inflammation are both related and become exacerbated in elderly people due to malfunction of antioxidant defense mechanisms (Nita and Grzybowski, 2016, Kimura et al., 2017). Oxidative stress and inflammation play, therefore, a key role in the initiation and progression of many different age-related

* Corresponding author.
E-mail address: carmen.alvarez.lorenzo@usc.es (C. Alvarez-Lorenzo).

https://doi.org/10.1016/j.ijpharm.2022.122281
Received 10 July 2022; Received in revised form 3 October 2022; Accepted 7 October 2022
Available online 13 October 2022

ocular diseases like surface disorders (keratoconus and corneal ectasia), macular degeneration, diabetic retinopathy (DR), cataract, glaucoma and uveitis, which can lead to progressive loss of vision and blindness without proper treatment (Behl et al., 2016; Ung et al., 2017; Dogru et al., 2018, Pinazo-Duran et al., 2018; Semeraro et al., 2019; Kang and Yang, 2020).

Considering all the above mentioned, a therapeutic strategy which targets ROS is required to prevent oxidative stress-related ocular diseases or slow down their progression. Indeed, the effectiveness of different antioxidants (vitamins, carotenoids, flavonoids, polyphenols, lutein, zeaxanthin and omega-3 fatty acids, among others) against some age-related ocular diseases including DR has already been demonstrated in animal models and humans (Kimura et al., 2017; Pinazo-Duran et al., 2018; Kang and Yang, 2020). Resveratrol (*trans*-3,5,4′-trihydroxystilbene) (Fig. 1) is a natural polyphenolic compound with antioxidant, radical scavenging, antiproliferative, antiangiogenic, anti-inflammatory, anti-apoptotic and vasodilating properties which may be useful for eye health (Bola et al., 2014; Ghadiri Soufi et al., 2015; Chen et al., 2019). In the specific case of DR, resveratrol acts through multiple molecular mechanisms, and different *in vitro* and *in vivo* studies (most of them using oral administration) have demonstrated its beneficial effects (Toro et al., 2019; Huang et al., 2020; Delmas et al., 2021). Moreover, resveratrol may act as prebiotic, restoring ocular microbiota and inhibiting biofilm development by opportunistic bacteria that cause ocular diseases (Petrillo et al., 2020). Despite its excellent potential, the clinical efficacy of resveratrol is compromised by its poor aqueous solubility (30 μg/mL), instability when exposed to light, and low oral bioavailability (<1 %) (Amri et al., 2012; Summerlin et al., 2015; Peñalva et al., 2018).

In the last few decades, polymeric micelles have become one of the most promising delivery systems of hydrophobic drugs for the treatment of anterior and posterior ocular diseases thanks to their mucoadhesive features and small size, which increases the contact with the ocular surface and facilitates drug penetration across cornea and sclera, enhancing ocular bioavailability without interfering with vision (clear solution) (Mandal et al., 2017; Grimaudo et al., 2019; Durgun et al., 2020). So far, resveratrol-loaded Soluplus® micelles have been tested to promote *in vivo* corneal wound healing (Li et al., 2020).

Bovine milk protein micelles are attracting increasing attention as drug nanocarriers since they combine widely available natural sources, capability to transport poorly soluble molecules (natural transporters of calcium phosphate) and activity as radical scavengers (Kimpel and Schmitt, 2015; Rehan et al., 2019). Casein (Fig. 1) represents a family of phosphoproteins which constitutes approximately 80 % of all bovine milk proteins. Casein is sensitive to pH and precipitates at its isoelectric point of 4.6 (Phadungath, 2005). It is made up of αs1-casein, αs2-casein, β-casein, and κ-casein (Phadungath, 2005; Glab and Boratyński, 2017; Rehan et al., 2019). The αs- and β-caseins are highly phosphorylated and precipitate with excess Ca^{2+} ions. Differently, κ-caseins protect other caseins from precipitation, which makes casein micelles more stable. In fact, in milk about 80–95 % of the casein is forming part of spherical micelles (50–500 nm; 10^6-10^9 Da) made of a 94 % of protein and a 6 % of colloidal calcium phosphate (Phadungath, 2005; Rehan et al., 2019) although the exact conformation is still unknown. Casein micelles-based systems have been tested for the delivery of metformin (Raj and Uppuluri, 2015), celecoxib (Turovsky et al., 2015a, 2015b; Bachar et al., 2012), doxorubicin (Gandhi and Roy, 2019), ibuprofen (Turovsky et al., 2015a, 2015b) and mitoxantrone (Shapira et al., 2010). The studies regarding interactions of casein with resveratrol are still limited (Bourassa et al., 2013) and mainly focused on its oral administration searching for antitumoral action (Peñalva et al., 2018). To the best of our knowledge, encapsulation of resveratrol or other compounds in casein micelles for ocular delivery has not been investigated yet. It has been shown that β-casein may form mixed micelles with Pluronic® F127 copolymer (Lutrol F127; Fig. 1), which could be useful to shield the ionic charges of the protein and to confer stealth properties (Portnaya et al., 2011). Pluronics or poloxamers are amphiphilic linear polymers of poly (ethylene oxide)-poly(propylene oxide)-poly(ethylene oxide) (PEO-PPO-PEO) widely tested for ocular formulations and some drug products in the market contain poloxamers as main excipients (EMA, 2022). Advantages of mixed micelles are related to lower critical micelle concentration (CMC) and enhanced stability against both physical and chemical agents (Ribeiro et al., 2012; Del Regno et al., 2021).

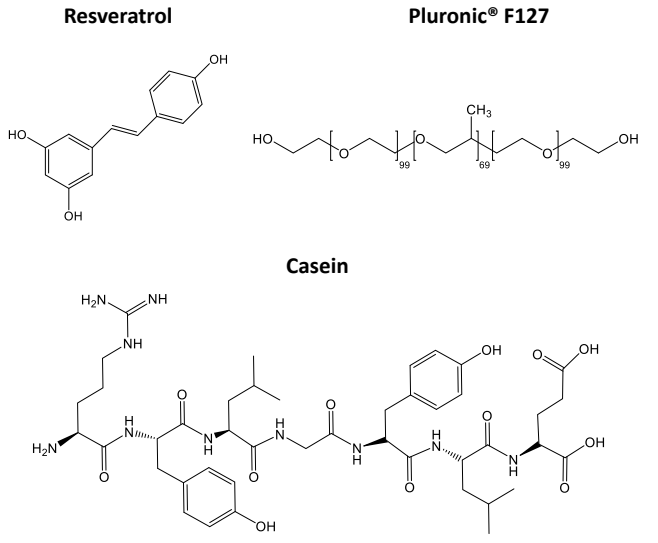

Fig. 1. Chemical structure of *trans*-resveratrol, Pluronic® F127, and casein.

The present work relies on the hypothesis of that Pluronic® F127 micelles and Pluronic® F127/casein mixed micelles may lead to nanocarriers with enhanced capability to encapsulate resveratrol, to preserve its antioxidant features and to facilitate its penetration through the ocular structures. Thus, the aim was to prepare and characterize single and mixed micelles of Pluronic® F127 and casein (Table 1) and to evaluate their suitability as resveratrol nanocarriers for ocular treatments. The micelles were characterized regarding size, zeta potential, and ability to solubilize and stabilize resveratrol. The most promising formulations were evaluated in terms of *ex vivo* porcine corneal and scleral permeability of resveratrol, antioxidant capacity, rheological behavior, mucoadhesion, and ability to inhibit the growth of two bacteria commonly involved in eye infections, *Pseudomonas aeruginosa* and *Staphylococcus aureus*. After preliminary screening of biocompatibility using the Hen's Egg Test on the Chorioallantoic Membrane (HET-CAM) assay (ICCVAM, 2010) and the fish embryo toxicity test (FET) on a zebrafish model (Hering et al., 2020), the most suitable formulation was evaluated *in vivo* (rabbit model) regarding its safety, permanence on the ocular surface, and access of resveratrol to eye tissues.

2. Materials and methods

2.1. Materials

Casein from bovine milk purified powder (C-5890), phosphate buffer saline 10x concentrate (BioPerformance Certified, suitable for cell culture; P5493), and 2,2-diphenyl-1-picrylhydrazyl (DPPH) were purchased from Sigma-Aldrich (St. Louis, MO, USA). Kolliphor® P 407 (Lutrol F127) was from BASF ChemTrade GmbH (Burgbernheim, Germany). Resveratrol (228.24 g/mol, solubility 30 μg/mL water, Log P 3.10) was from ChemCruz Santa Cruz Biotechnology Inc. (Dallas, TX, USA). Propylene glycol (PPG, 76.06 g/mol; purity 99.94 %) was from Guinama (Valencia, Spain). Disodium hydrogen phosphate anhydrous (Na_2HPO_4) was from Acofarma (Barcelona, Spain). Potassium chloride (KCl) and Luria Bertani (LB) broth were from Scharlab S.L. (Barcelona, Spain). Sodium dihydrogen phosphate anhydrous (NaH_2PO_4) and

Table 1
Composition of Pluronic® F127 (P), Pluronic® F127/casein (PC) and casein (C) formulations prepared in phosphate buffer pH 7, and size (by number), polydispersion index (PDI), and Z-potential after resveratrol loading (mean values ± standard deviations). The pH of the formulations ranged from 7.0 to 7.3. The letter R at the end of the formulation code refers to resveratrol loading (loading values are provided in Table 2).

Formulation	Pluronic® F127 (%)	Pluronic® F127 (mM)	Casein (%)	Size (nm)	PDI	Z-Pot (mV)
P2.5R	3.15	2.5	–	3.6 ± 0.3	0.3 ± 0.1	−1.5 ± 1.3
P5R	6.3	5	–	3.1 ± 0.5	0.5 ± 0.1	−0.1 ± 0.1
P7.5R	9.45	7.5	–	3.1 ± 0.1	0.5 ± 0.0	−0.9 ± 0.8
P10R	12.6	10	–	2.7 ± 0.2	0.6 ± 0.2	0.0 ± 0.4
P15R	18.9	15	–	2.1 ± 0.2	0.3 ± 0.1	−0.3 ± 0.2
PC2.5R	3.15	2.5	0.1	10.9 ± 11.3	1.1 ± 0.1	−17.0 ± 0.7
PC5R	6.3	5	0.1	32.7 ± 5.2	0.8 ± 0.0	−9.6 ± 1.3
PC7.5R	9.45	7.5	0.1	2.6 ± 0.8	0.8 ± 0.1	−4.4 ± 0.6
PC10R	12.6	10	0.1	2.4 ± 0.8	0.9 ± 0.0	−2.2 ± 0.5
PC15R	18.9	15	0.1	2.4 ± 0.2	1.0 ± 0.6	−0.2 ± 0.2
CR	–	–	0.1	23.0 ± 5.0	0.4 ± 0.0	−10.5 ± 2.3

sodium chloride (NaCl) were from Labkem (Barcelona, Spain). Sodium bicarbonate ($NaHCO_3$) was from Probus S.A. (Barcelona, Spain). Calcium chloride dihydrate ($CaCl_2{\cdot}2H_2O$) was from Merck KGaA (Darmstadt, Germany). Ethanol absolute 99.9 % and sodium hydroxide (NaOH) were from VWR Chemicals (Fontenary-Sous-Bois, France). Tryptic soy broth (TSB) was from Scharlau (Barcelona, Spain). Ultrapure water (resistivity > 18.2 MΩ·cm) was obtained by reverse osmosis (MilliQ®, Millipore Ibérica, Madrid, Spain). Simulated lachrymal fluid (SLF) was prepared with 6.78 g/L NaCl, 2.18 g/L $NaHCO_3$, 1.38 g/L KCl and 0.084 g/L $CaCl_2{\cdot}2H_2O$ (Paulsson et al., 1999; Alvarez-Rivera et al., 2019) and the pH was adjusted to 7.5. TSB-1 medium was prepared with 6 g of TSB and 1 g of NaCl for 200 mL. LB medium was prepared with 5 g of LB for 200 mL.

2.2. Single and mixed micelles preparation

Casein solution (0.4 %w/w; 200 mL) was prepared by adding slowly (to avoid denaturalization) the corresponding amount of casein to phosphate buffer pH 7 (3.05 mM NaH_2PO_4 and 5.65 mM Na_2HPO_4) at 29 °C and kept at 200 rpm for 24 h (Portnaya et al., 2011). Pluronic® F127 dispersions (25.2, 16.8, 12.6, 8.4 and 4.2 %w/w; 50 mL) were prepared in duplicate in phosphate buffer pH 7, kept under magnetic stirring at 300 rpm for 5 h in an ice bath and stored at 4 °C until the next day to ensure the complete dispersion of the copolymer. The next day, after 1 h under magnetic stirring in an ice bath at 300 rpm, 16.67 mL of phosphate buffer pH 7 or of casein (0.4 %) solution were added to the Pluronic® dispersions to obtain finally 66.67 mL of each formulation with the composition indicated in Table 1. All systems were magnetically stirred at 300 rpm for 7–8 h in an ice bath to facilitate the mixing and to avoid the gelling of the dispersions with higher content in Pluronic®. All dispersions were kept in the fridge until use. Pluronic® F127 and casein single micelles were coded as P and C, respectively, while Pluronic® F127/casein mixed micelles were coded as PC followed by the concentration (mM) of Pluronic® F127.

2.3. Micelle size, zeta potential and pH

Particle size, size distribution, PDI and zeta potential of non-loaded (n = 2) and resveratrol-loaded (n = 3) micelle dispersions were measured in a Zetasizer® Pro-Blue (Malvern Instruments, UK; refractive index 1.33 and detector angle 173°, back scatter) at 10 and 35 °C; dispersions prepared with the highest content in Pluronic® F127 were only evaluated at 10 °C to avoid gel formation. The dispersions were measured directly without dilution. Folded capillary cuvettes (DTS1070) were used for the measurements. The pH was measured with a GLP22 pH meter (Crison Instruments, Spain) at room temperature and at 35 °C at least in duplicate.

2.4. Solubility study

Aliquots (10 mL) of each micelle dispersion were poured in 50 mL Falcon® tubes to which resveratrol was added in excess (approximately 100 mg). Solubility of resveratrol in phosphate buffer pH 7 was tested in parallel. All systems were maintained under magnetic stirring (300 rpm) in an ice bath for 3 days and then centrifuged (Eppendorf® 5804R, Germany) at 5 °C and 4,000 rpm for 30 min. Absorbance of the supernatants was measured at 305 nm (UV–Vis spectrophotometer Agilent 8453, Germany) previous dilution of aliquots (100 μL) of each dispersion in ethanol:water 50:50 v/v medium. Resveratrol concentration was calculated from the absorbance using a previously validated calibration curve.

Resveratrol solubility data were used to estimate the molar solubilization capacity (χ; Eq. (1)), the micelle-water partition coefficient (P; Eq. (2)), the molar micelle-water partition coefficient (PM; Eq. (3)) for a copolymer concentration of 1 M, the standard-free Gibbs energy of solubilization (ΔGs; Eq. (4)), and the proportion of drug molecules encapsulated in the micelles (Eq. (5)) as follows (Rangel-Yagui et al., 2005):

$$\chi = \frac{S_{tot} - S_w}{C_{copol} - CMC} \tag{1}$$

$$P = \frac{S_{tot} - S_w}{S_w} \tag{2}$$

$$PM = \frac{\chi \cdot (1 - CMC)}{S_w} \tag{3}$$

$$\Delta Gs = -RTln(PM) \tag{4}$$

$$m_f = \frac{S_{tot} - S_w}{S_{tot}} \tag{5}$$

In these equations, S_{tot} represents the total solubility of resveratrol in the micellar solution, S_w the solubility of resveratrol in phosphate buffer pH 7, C_{copol} is the copolymer concentration in each micellar solution, and R is the universal constant of gases.

2.5. Stability of loaded and non-loaded micelles

Formulations were stored at 4 °C, protected from light to avoid resveratrol degradation, and monitored over 30 days regarding pH, size, polydispersion index and Z-potential. The amount of resveratrol within the micelles was also monitored as indicated above. Stability against dilution was evaluated by pouring aliquots of resveratrol-loaded micelle

dispersions (30 μL) into quartz cells at 35 °C already containing 2970 μL of SLF (total volume 3000 μL). The 100-fold diluted dispersion was gently shaken, and the absorbance measured at 305 nm every 30 s for 30 min (UV–Vis spectrophotometer Agilent 8453, Germany). All experiments were carried out at least in duplicate.

2.6. Rheological characterization

The storage (G′) and loss (G″) moduli of micelle dispersions with and without resveratrol were recorded in a Rheolyst AR-1000 N (TA Instruments, UK) rheometer fitted with a Peltier plate and a cone (60 mm, 2.1°) as a function of temperature (10–45 °C). The oscillation stress was fixed at 0.1 Pa and the angular frequency at 5 rad/s.

2.7. HET-CAM assay and FET test using a zebrafish model

The ocular irritation potential of micelles with and without resveratrol was tested using the HET-CAM assay as previously described (Alvarez-Rivera et al., 2016). After 8 days of incubation of the fertilized hens' eggs (50–60 g, Coren, Spain) in a climatic chamber at 37 °C and 60 % relative humidity, a circular cut (1 cm in diameter) was made on the eggshell to remove the inner membrane and expose the chorioallantoic membrane (CAM). Then, aliquots (200 μL) of each formulation were directly poured on the CAM. 0.9 % NaCl and 0.1 N NaOH solutions were used as negative and positive controls, respectively. CAM vessels were monitored for 5 min and the time at which hemorrhage, vascular lysis or coagulation occurred was recorded to calculate the irritation score (IS) as previously reported (ICCVAM, 2010). According to the IS values obtained, formulations were classified as non-irritant (IS $<$ 1), mildly irritant (1 $\leq$ IS $<$ 5), moderately irritant (5 $\leq$ IS $<$ 10), or severely irritant (IS $>$ 10). The assay was carried out in duplicate and independently for each formulation.

A fish embryo toxicity test (FET) was performed to elucidate the effect of blank and resveratrol-loaded (0.4 mg/mL) formulations on the development of zebrafish (*Danio rerio*) embryos following the Organization for Economic Co-operation and Development normative (OECD, 2006). The zebrafish embryos employed for this study were from the fish facilities of the Department of Genetics of the University of Santiago de Compostela. They were raised in aquarium systems (28 °C, pH = 7) with a photoperiod of 14 h of light and 10 h of darkness. Fertilized zebrafish eggs before 5 h post-fecundation (hpf) were placed into 96-well cell culture plates (1 embryo per well; 16–17 wells in triplicate) and then the formulations (10 μL) were added to the medium (190 μL). For these tests, the Pluronic®/casein dispersions were autoclaved (121 °C, 20 min) before adding resveratrol. As negative controls, 20 embryos were grown, in triplicate, in sterilized reverse osmosis water in the absence of any formulation. 3,4-Dichloroaniline was used as positive control. The experiment was carried out in triplicate for 96 h, and the four lethal effects indicated in FET (coagulation of the embryo, absence of somite formation, absence of separation of the tail from the yolk, and absence of heartbeat) were monitored each 24 h. To be a valid test, the mortality of zebrafish embryos in the negative control after 96 h must not exceed 10 %, and the mortality in the positive control (3,4-dichloroaniline) must be at least 30 %. In all tests the mortality of control embryos was 0.0 % and the mortality under presence of 3,4-dichloroaniline was 100.0 %. Thus, both criteria were fulfilled.

2.8. Antioxidant properties

The antioxidant activity of resveratrol in phosphate buffer pH 7 and in all micelle formulations was quantified, in triplicate, by using a modified DPPH assay (Vivero-Lopez et al., 2021a). Micelles without resveratrol were used as controls. An aliquot of each dispersion (0.1 mL) was mixed with 4.5 mL of ethanol and 0.4 mL of a freshly prepared 0.4 mM DPPH solution in ethanol and vortexed for 5 s. After 30 min of incubation in the dark, the absorbance was measured at 517 nm (UV–Vis spectrophotometer Agilent 8534, Germany). The free radical scavenging activity was expressed as a) μg/mL of DPPH in the reaction medium by interpolation into a validated calibration curve performed with DPPH in ethanol (5.91–31.55 μg/mL), and b) percentage of scavenging activity (Vivero-Lopez et al., 2021a).

2.9. Ability to inhibit bacterial growth

Non-loaded and resveratrol-loaded P5, P10, P15, PC5, PC10, PC15 micelles as well as resveratrol solutions in ethanol:water 50:50 v/v medium were tested regarding their capability to inhibit the growth of *Pseudomonas aeruginosa* PAO1 (Lausanne sub-line, donated by M. Cámara, Univ. of Nottingham, Nottingham, UK) and *Staphylococcus aureus* ATCC25923 (ATCC, Manassas, VA, USA). The effect of the dilution of the culture medium with ethanol and PBS was also studied to elucidate the inhibitory bacterial growth due exclusively to resveratrol and to the formulations. All experiments were carried out at least in sextuplicate. As control, bacterial growth with no resveratrol or dispersions in the culture medium was monitored.

Pre-inocula and inocula preparation was carried out according to previously described protocols with slight modifications (Vivero-Lopez et al., 2021a, Vivero-Lopez et al., 2021b). The optical density of the inocula was adjusted to 0.05 for *S. aureus* in TSB-1 and to 0.01 for *P. aeruginosa* in LB after measuring the optical density of centrifuged (13,000 rpm, 3 min) and resuspended (1 mL of fresh medium) pre-inocula. The inocula were gently homogenized and divided among 96-well cell culture plates. All procedures were performed in a biological safety cabinet under sterile conditions.

First, the capacity of resveratrol at different concentrations (10, 50, 100, 200 and 300 μg/mL) in ethanol:water 50:50 v/v to inhibit bacteria growth was evaluated. Concentrated (3000, 2000, 500 and 100 μg/mL) resveratrol solutions in ethanol:water 50:50 v/v were filtered (Biofil® Syringe Filter, 0.22 μm PES membrane) and added (10–20 μL) to a 96-well plate containing the inoculum (180 μL or 180 μL + 10 μL ethanol:water 50:50 v/v) (10- or 20-fold dilution; final ethanol concentration 5 %). Wells with bacteria inoculum (200 μL), bacteria inoculum (180 μL) plus ethanol:water 50:50 v/v (20 μL), and medium without bacteria (200 μL) were also prepared (n = 6). The capacity of single and mixed micelle dispersions was also evaluated by adding 20 μL of each one to wells of a 96-well plate containing 180 μL of the corresponding inoculum bacteria. Then, the plates were incubated protected from light for 24 h at 37 °C without stirring and optical densities of all wells were measured at predetermined times (0, 2, 4, 6, 8 and 24 h) at 595 nm in a plate reader (FLUOstar optima, BMG LabTech, Ortenberg, Germany). Before each measurement, the wells were shaken to homogenize the suspension and avoid aggregates that could interfere with the measurement.

2.10. Ex vivo corneal and scleral permeability tests

Resveratrol corneal and scleral permeability tests were carried out for P10R and PC10R formulations (resveratrol concentration 9 mg/mL), at least in triplicate, following a previously described protocol (Varela-Garcia et al., 2020). Fresh porcine eyes of male and female Pietrain, Duroc and Belgian white pigs (6–8 months, 100 Kg weight) obtained from a local slaughterhouse were transported immersed in PBS in an ice bath. Then, isolated scleras and corneas were washed with PBS, visually inspected to assess the absence of any tissue damage (cuts, cracks or opacification), and fitted into Franz diffusion cells filled with a mixture of propylene glycol (PPG):water 40:60 v/v medium. The receptor medium (6 mL) was kept at 37 °C under gentle magnetic stirring (400 rpm) avoiding bubble formation. After equilibration (30 min), the medium of the donor chambers (PPG:water 40:60 v/v) was removed and replaced by the formulations (1 mL). The area available for permeation was 0.785 cm^2. The donor chambers were covered with parafilm and protected from light. The corneal curvature was not preserved during the

experiment due to the design of Franz cells and to ensure a proper contact between the tissue and the liquid in both donor and receptor chambers. The permeation area comprised the central zone of the cornea without the limbus.

After 30 min of applying the formulation and then every hour for 6 h, 1 mL of the receptor medium was taken and replaced with the same volume of PPG:water 40:60 v/v, taking care of removing any bubble from the diffusion cells. The steady state flux (J), the apparent permeability coefficient (P_{app}) and lag time were calculated as previously reported (Cabrera-Pérez et al., 2015; Alvarez-Rivera et al., 2016).

A JASCO (Tokyo, Japan) HPLC fitted with a C18 column (Waters Symmetry, 5 μm, 4.6 × 250 mm) and operated with ChromNAV software (ver. 2.2.8.5, JASCO, Tokyo, Japan) was used to quantify the amount of resveratrol permeated through and accumulated into the tissues following a previously developed method (Vivero-Lopez et al., 2021a). The analysis was done by isocratic elution with a mobile phase of methanol:water 50:50 v/v at 1 mL/min and 35 °C using a run time of 8 min (retention time 4.6 min). The injection volume was 50 μL and the UV detector was set at 305 nm. Two different calibration curves of resveratrol in methanol:water 50:50 v/v (0.05–2 and 1–6 μg/mL) were used to validate the method regarding linearity (correlation coefficient, $r^2 > 0.9997$), accuracy (coefficient of variation of the response factors < 1.3 %) and precision (coefficients of variation of repeated measurements < 1.3 %). The percentages of recovery were in the 99–101 % range. The detection and quantification limits were 0.007 and 0.016 μg/mL, respectively. Resveratrol peaks recorded for the same resveratrol concentration prepared in PPG:water 40:60 and ethanol:water 50:50 v/v overlapped showing the same area and peak shape. Thus, the same calibration curves were used for resveratrol permeation and retention analysis.

Aliquots of the donor chambers were collected after 6 h of assay to quantify the amount of resveratrol remnant. The corneas and scleras were visually inspected to verify that none of them had cracks or modifications, and the surface area exposed to the formulation was cut and placed in Falcon® tubes with 3 mL of ethanol:water (50:50 v/v) at 37 °C. After 24 h, they were sonicated for 99 min at 37 °C, centrifuged (1000 rpm, 5 min, 25 °C), and the supernatant was filtered (PTFE hydrophilic, Syringe Filter, 0.22 μm 13 mm; Scharlab S.L., Spain), centrifuged again (14,000 rpm, 20 min, 25 °C), and filtered again to be analyzed by HPLC as described above. Absence of interferences caused by the filter in the quantification method was verified. Resveratrol stability in contact with the ocular tissues was confirmed as no differences were observed between the HPLC chromatograms (no changes in area and retention time, no new peaks) registered for resveratrol before and after being in contact with the ocular tissues for 6 h at 37 °C.

The procedure to extract resveratrol from cornea and sclera was validated by incubating fresh tissue pieces of the same size as the hole available for permeation in the Franz cell in separate Falcon® tubes (n = 3) containing 6 mL of a 0.4 mg/mL resveratrol in PPG:water 40:60 v/v solution. The tubes were incubated protected from light at 37 °C and 180 rpm for 6 h. Then, the tissues were immediately transferred to new Falcon® tubes containing 3 mL of ethanol:water 50:50 v/v and incubated under gently stirring at 37 °C. Subsequent sonication, centrifugation and filtration were carried out as described above. The percentages of recovery were calculated by dividing the amount of resveratrol extracted in the ethanol:water 50:50 solution by the amount of resveratrol absorbed by the tissues, calculated from the difference between the initial (t = 0 h) and final (t = 6 h) amount of resveratrol in the Falcon® tubes. The amounts of resveratrol were calculated from the areas obtained by HPLC considering a previously validated calibration curve and the volumes of the different steps (6 and 3 mL). An extraction procedure cutting the tissues after the initial 6 h step was also carried out to evaluate if this step could increase the percentage of recovery obtained. No differences in the percentages of recovery were observed between cutting (103 ± 8 % and 89 ± 18 % for cornea and sclera) or not the tissues (116 ± 17 % and 80 ± 6 % for cornea and sclera) so the extraction procedure was carried out without cutting the tissues after the permeability assay.

2.11. Mucoadhesion tests

The mucoadhesive properties of the most promising formulations (P10R and PC10R) were evaluated using a TA.XT Plus Texture analyzer (Stable Micro Systems Products, UK) following a previously described protocol with some modifications (Lorenzo-Veiga et al., 2020). To carry out the test, fresh porcine corneas and scleras were fixed to the probe of the texturometer, and 50 μL of each formulation were placed at the bottom of a container maintained at 35 °C to simulate eye drop instillation. The texturometer probe descended at 1 mm/s, and mucoadhesion strength was determined as the detachment force needed to separate the tissue from the formulation after applying a force of 0.5 N for 60 s. For each tissue, mucoadhesion was alternatively recorded for the formulation and for control PBS pH 7 (5 cycles) in order to evaluate possible changes due to multiple cycles of compression. The experiment was carried out in duplicate for each formulation and tissue.

2.12. In vivo experiments

In vivo experiments were carried out fulfilling 3R's principles and following the Association for Research in Vision and Ophthalmology (ARVO) Statement for the Use of Animals in Ophthalmic and Vision Research and the European Directive 2010/63/EU, with the permission of the Committee for Animal Experimentation of the University Complutense of Madrid [code O00023280e2100023620]. Four male New Zealand white rabbits (age approx. 3 months, 3.97 ± 0.73 Kg weight) were stabled in individual cages with free access to food and water at 18 °C and 50 % relative humidity inside a light-controlled room with 12 h light–dark cycles. A single drop (50 μL) of a P10R formulation loaded with resveratrol (4 mg/mL) was gently instilled in the lower conjunctival sac of the right eye using a micropipette. Left eyes served as controls. The ocular surface of the rabbits was carefully observed with a VX75 slit lamp (Luneau Technology, Chartres, France) before (t = 0 h) and after (t = 8 h) the administration of the formulation. Samples of tear fluid were collected at 5, 15 and 30 min, and every hour until 8 h using Schirmer test strips, which were placed in the tarsal conjunctiva of the inferior lid for 10 s with closed eyes to avoid the reflex secretion associated with blinking. The volume collected was calculated as a function of the millimeters of wetted strip. No animals or data were discarded, and no adverse events were observed.

Resveratrol in the tear fluid was quantified after extraction of the test strips with ethanol:water 50:50 v/v solution (200 μL in 1.5 mL Eppendorf® tubes). The tubes were vortexed for 1 min, maintained protected from light at 4 °C for 15 h, and vortexed again for 2 min. Then, the strips were removed from the tubes, and the tubes were heated at 98 °C for 2 min, placed in an ice bath for 10 min and centrifuged at 13,000 rpm for 10 min at 25 °C for protein denaturation. Finally, the supernatants were collected and stored at −80 °C until HPLC analysis (as in section 2.10). The extraction and protein denaturation methods were shown to recover>98 % resveratrol present in the strips.

At the end of the experiment (8 h) the rabbits were euthanized (i.v. injection of propofol 0.75 mL/Kg and pentobarbital sodium 0.5 mL/Kg), and the aqueous humor was directly extracted from the anterior chamber of both eyes with a 25G needle and kept in 1.5 mL Eppendorf® tubes. The vitreous humor was also separated. Cornea, crystalline lens, sclera and retina were dissected and incubated with ethanol:water 50:50 v/v (500 μL, 500 μL, 800 μL and 200 μL, respectively) in 1.5 mL Eppendorf® tubes. Then, resveratrol extraction and protein denaturation were carried out as described above. The supernatants were stored at −80 °C. Before UPLC analysis all samples were diluted 1.5 times with acetonitrile and mixed using an Automated Liquid Handling System, Caliper Zephyr, 3 cycles of 50 μL at 78 μL/s. The plate was then centrifuged at 3700 rpm at 4 °C for 30 min. Quantification of resveratrol

in the different tissues was carried out using a Waters Acquity UPLC H-Class coupled with a Xevo TQD MS System fitted with an HypersilGOLD C18 column (1.9 μm 2.1 × 50 mm, Thermo-Fischer) at 35 °C. The analysis was done by gradient elution using water + 0.1 % formic acid as solvent A, and acetonitrile + 0.1 % formic acid as solvent B, as follows: 0–0.1 min 5 % B, 0.1–1.0 min 5–100 % B, 1.0–2.0 min 100 % B, 2.0–2.1 min 100–95 % B, and 2.1–2.5 min 5 % B, and at a flow rate of 0.6 mL/min. Electrospray ionization (ESI) was run in positive mode with a source temperature of 150 °C and a desolvation temperature of 500 °C. Capillary voltage was set to 3 kV and the cone voltage was set to 45 V. Desolvation gas flow was 900 L/h and cone gas flow was set to 50 L/h. Resveratrol was monitored using multiple reaction monitoring (MRM)/ES+ mode precursor and product ion transition 229.045 > 106.993. The injection volume was 4 μL and the retention time was 1.18 min.

2.13. Statistical analysis

The statistical analysis was performed using the Statgraphics Centurion 18, v. 18.1.13 (StatPoint Technologies Inc., Warrenton VA, USA). Differences among formulations regarding biocompatibility, biofilm inhibition, mucoadhesion, and permeability through cornea and sclera were analyzed using ANOVA and multiple range tests. A statistical significance of 95 % ($p < 0.05$) was established in all the statistical tests, while the results were expressed as mean ± standard deviation (SD).

3. Results and discussion

3.1. Micelles preparation

Pluronic® F127 and casein were easily dispersed in phosphate buffer pH 7 at the chosen concentrations (Table 1). The highest Pluronic® F127 concentration was 15 mM to avoid gel formation at room temperature. Pluronic® F127 dispersions at high concentrations may be beneficial for increasing the permanence of the formulation in the ocular surface, but at the same time may hinder the solubilization process if the viscosity is too high during the processing (Taveira et al., 2018). The CMC for Pluronic® F127 has been reported to be 0.39 mM at 25 °C in phosphate buffers from surface tension measurements (Rodriguez-Perez et al. (2006)). Thus, for all dispersions, the Pluronic® F127 concentration (ranging from 2.5 to 15 mM) was above the CMC value. The CMC for casein has been reported to be approx. 0.1 % and specifically 0.03–0.07 % for β-casein depending on the pH, temperature, and ionic strength (Glab and Boratyński, 2017). The CMC at 29 °C in phosphate buffer was found to be 0.1368 % (0.057 mM) using isothermal titration calorimetry (ITC) (Portnaya et al., 2011). The commercial natural casein chosen for the present study was a mixture of α-s1 casein, α-s2 casein, β-casein, and κ-casein, and for comparative purposes the concentration was fixed at 0.1 %. In preliminary studies, we observed that dispersions prepared at higher concentrations underwent phase separation in few days. Assuming a molecular weight of 24,000 Da for casein, a casein concentration of 0.1 % was equal to 0.0416 mM. This concentration was previously shown to be able to form mixed micelles when a minimum concentration of 0.076 mM Pluronic® F127 was added (Portnaya et al., 2010). In those earlier studies, the CMC of the mixed micelles was estimated to be 0.1176 mM (slightly above the CMC of Pluronic® F127 solely, 0.096 mM, recorded by ITC). From that previous information, the formation of casein-Pluronic® F127 mixed micelles was assumed to occur also under the conditions tested in the present study.

3.2. Micelle size, zeta potential and pH

Size, polydispersion index and Z-potential of single and mixed micelles before (**Table S1 in Supplementary Material**) and after the loading with resveratrol were recorded at 10 °C (Table 1) and 35 °C (**Table S2**). The analysis of size by intensity distribution at 10 °C (**Figure S1**) showed multiple populations specially after the loading with resveratrol. In addition, the size of the micelles by intensity was larger because large particles scatter much more light than small particles, and the scattering intensity is proportional to the sixth power of the particle diameter based on the Rayleigh's approximation. However, the analysis of size by number (**Figure S2**) showed unimodal size distribution and smaller sizes for single and mixed micelles before and after the loading with resveratrol. The size of PC mixed micelles without resveratrol increased with increasing Pluronic® F127 content at 10 °C, but this trend was not observed after the loading with resveratrol and all loaded formulations had very close and smaller size values (Table 1), which suggests that resveratrol may enhance hydrophobic interactions inside the micelles making them to be more compact. All single micelles before and after being loaded with resveratrol showed almost the same size at 35 °C, which means that resveratrol loading did not affect the size at 35 °C (**Table S2**). As expected, the Z-potential of Pluronic® F127 micelles was close to zero (Portnaya et al., 2011). Differently, casein micelles had strongly negative surface since the pH of the medium was above the isoelectric point of the protein. Namely, casein molecules are formed by a short highly charged domain and a long hydrophobic segment, which favors their self-assembly (Phadungath, 2005). Mixed micelles showed lower absolute values (less negative) as the concentration in Pluronic® increased (Table 1 and **Table S1 and S2**). The same trend was observed for mixed micelles of α-casein and PEG400 (Kessler et al., 2014). This finding indicated that Pluronic® F127 successfully hided protein charges, probably by the shielding with the PEO chains (Portnaya et al., 2011).

The pH values registered for all dispersions at both temperatures and loaded or not with resveratrol, were very close to the pH of the phosphate buffer in which they were prepared and showed no modification due to the Pluronic® F127, casein or resveratrol addition. Moreover, the pH values close to physiological tear value (6.5–7.6) may ensure good ocular tolerance and resveratrol stability (Robinson et al., 2015).

3.3. Solubility study

Resveratrol has previously been loaded in nanoparticles, β-cyclodextrins and Soluplus® micelles for topical ocular administration (Pandian et al., 2017; Dinte et al., 2020; Li et al., 2020), but there were no studies on the capability of Pluronic® F127 and Pluronic® F127/casein mixed micelles to solubilize resveratrol for ophthalmic applications.

Solubility of resveratrol in phosphate buffer pH 7 was 16.31 ± 1.55 μg/mL (~0.07 mM), a value slightly lower than the values previously reported in the literature (21 μg/mL) probably because the lower working temperature (10 °C vs. 37 °C) (Cadena et al., 2013). Both, single and mixed micelles increased the apparent solubility of resveratrol (Table 2). Since Pluronic® F127 was the major species in the dispersion, for comparative purposes the estimation of χ, PM, and ΔG of the mixed micelles was made assuming a CMC value similar to that of single Pluronic® F127, i.e., 0.39 mM, which was slightly higher than that found by ITC (0.1176 mM) (Portnaya et al., 2011).

The highly negative free energy of solubilization indicated that solubilization of resveratrol in the micelles occurred spontaneously. Casein single micelles had low solubilization capability and most resveratrol remained free in solution. Differently, Pluronic® F127 single and mixed micelles notably enhanced the apparent solubility, and the increase was higher as Pluronic® F127 concentration raised, as previously reported for other Pluronic® F127 mixed micelles (Katekar et al., 2020). This could be due to a stable interaction between the aromatic ring in resveratrol and the propylene oxide groups in Pluronic® F127 (Jadhav et al., 2016, Katekar et al., 2020). However, the highest solubility was recorded for 10 mM Pluronic® F127 both as single micelles and as mixed micelles. Probably the increase in viscosity, even at low temperature, observed for 15 mM Pluronic® F127 was behind the observed plateau (Taveira et al., 2018). Both Pluronic® single and mixed micelles showed partition coefficient values well above 1 indicating an efficient

Table 2
Resveratrol apparent solubility in single and mixed micelles and solubilization parameters estimated using equations 1–5. Solubility of resveratrol in phosphate buffer pH 7 was 16.31 ± 1.55 μg/mL. χ, molar solubilization capacity; P, partition coefficient; PM, molar partition coefficient; ΔG, free energy of solubilization; mf, molar fraction of drug encapsulated inside the micelle (mean values ± standard deviations).

Formulation	Solubility (mg/mL)	Solubility (mM)	χ	P	PM	ΔG (KJ/mol)	mf
P2.5R	0.17 ± 0.02	0.72 ± 0.11	0.31 ± 0.05	9.1 ± 1.5	2.64 ± 0.44	−2384 ± 394	0.90 ± 0.01
P5R	0.65 ± 0.29	2.85 ± 1.25	0.60 ± 0.27	38.8 ± 17.5	5.14 ± 2.32	−3895 ± 1060	0.97 ± 0.01
P7.5R	4.33 ± 0.77	19.0 ± 3.4	2.66 ± 0.47	264.3 ± 46.9	22.7 ± 4.0	−7703 ± 449	1.00 ± 0.00
P10R	8.14 ± 0.41	35.7 ± 1.8	3.71 ± 0.19	498.2 ± 25.3	31.6 ± 1.6	−8551 ± 127	1.00 ± 0.00
P15R	7.71 ± 0.52	33.8 ± 2.3	2.31 ± 0.16	471.7 ± 32.1	19.7 ± 1.34	−7376 ± 172	1.00 ± 0.00
PC2.5R	0.23 ± 0.14	1.02 ± 0.60	0.45 ± 0.28	13.2 ± 8.4	3.82 ± 2.43	−3016 ± 1444	0.91 ± 0.04
PC5R	1.33 ± 0.06	5.85 ± 0.25	1.25 ± 0.05	80.8 ± 3.5	10.69 ± 0.46	−5866 ± 105	0.99 ± 0.00
PC7.5R	4.39 ± 0.31	19.2 ± 1.4	2.70 ± 0.19	268.2 ± 18.9	23.01 ± 1.62	−7762 ± 177	1.00 ± 0.00
PC10R	9.36 ± 0.07	41.0 ± 0.3	4.26 ± 0.03	572.8 ± 4.3	36.36 ± 0.27	−8899 ± 18	1.00 ± 0.00
PC15R	8.14 ± 0.30	35.7 ± 1.3	2.44 ± 0.09	497.9 ± 18.6	20.79 ± 0.79	−7513 ± 93	1.00 ± 0.00
CR	0.02 ± 0.00	0.08 ± 0.01	−0.02 ± 0.01	0.12 ± 0.08	−0.29 ± 0.19	–	0.10 ± 0.06

incorporation of resveratrol to the micelle cores, with increases in resveratrol apparent solubility of up to 50 and 57 times, respectively. These values were in the range or even larger than those reported for Soluplus® (3.3 to 10 %) micelles that solubilized 1.67 to 4.44 mg resveratrol per mL (Li et al., 2020). It should be noted that an ophthalmic formulation of resveratrol at concentration of 1 mg/mL (encapsulated in PEG-chitosan nanoparticles) has demonstrated therapeutically relevant ocular effects, notably decreasing intraocular pressure (Pandian et al., 2017). Therefore, this concentration threshold can be readily fulfilled even with 5 mM Pluronic® when formulated as mixed micelles **(**Table 2**)**.

3.4. Stability of loaded and not loaded micelles

Pluronic® F127 single micelle dispersions kept their size constant over the 30 days of storage **(Figure S3)**. Differently, some changes in size were recorded for micellar systems composed of casein and Pluronic® F127, especially for non-loaded micelles. Incorporation of resveratrol into the micelles increased their physical stability. PDI values were around 0.4–1 for all formulations **(Figure S4)**. Changes in Z-potential **(Figure S5)** as well as in pH values **(Figure S6)** were minor. The amount of resveratrol incorporated into the micelles remained constant over the whole 30-day period **(**Fig. 2**)**. Thus, the formulations can be safely stored in the fridge at 4 °C protected from light.

Since ocular formulations undergo strong dilution once they enter in contact with the lachrymal fluid, the capability of all formulations to retain resveratrol once abruptly diluted was evaluated. The absorbance values remained higher for formulations that loaded higher amounts of resveratrol, and the values were almost constant during 30 min after dilution **(Figure S7)** which evidenced that resveratrol remained encapsulated in the micelles.

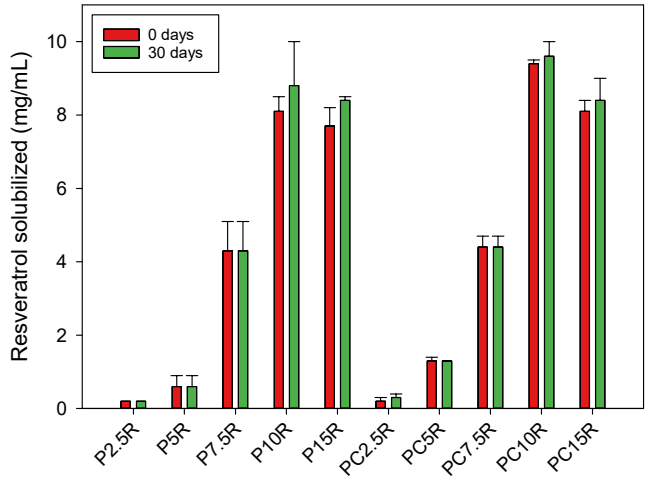

Fig. 2. Resveratrol solubilized into single and mixed micelles before (time 0 days) and after 30 days storage at 4 °C protected from light.

3.5. Rheological behavior

Rheological properties of eyedrops should show a good balance between easy instillation and prolonged retention on the ocular surface. *In-situ* gelling polymers, such as Pluronic® F127, may be advantageous in this regard (Al Khateb et al., 2016, Nagai et al., 2020). The sol–gel transition of unloaded and loaded single and mixed dispersions with a 5, 10 and 15 mM content in Pluronic® F127 was evaluated as a function of temperature **(**Fig. 3**)**. P and PC dispersions with 5 mM Pluronic® F127 showed negligible G′ values in the 10–45 °C interval performing as a free-flowing liquid-like system in good agreement with previous reports (Di Donato et al., 2020). Differently, all other dispersions showed an increase in G′ and G″ values as temperature raised. For non-loaded P10 and P15 dispersions **(**Fig. 3 **A,B)** a marked increase in G′ and G″ occurred when the temperature reached 26.7 °C and 20.3 °C, respectively; the gel point (cross-over point of G′ and G″) values were 28.2 °C and 21 °C respectively. The same trend was observed for the mixed micelles showing an increase in G′ and G″ values above 26.4 °C and 19.9 °C and temperature gel points of 27.5 °C and 20.6 °C for PC10 and PC15, respectively. In addition, the loading of these dispersions with resveratrol **(**Fig. 3 **C,D)** led to a decrease in the gel point for single (23.9 °C and 15.2 °C) and mixed micelles (27.1 °C and 15.2 °C) with a content in Pluronic® F127 of 10 and 15 mM respectively. This means that the encapsulation of hydrophobic resveratrol favors dehydration and gel transition as was previously observed with other drug molecules like naproxen and indomethacin (Sharma and Bhatia, 2004). No relevant differences were observed between P and PC mixed dispersions suggesting no significant effects on the rheological behavior due to the incorporation of casein. Considering all the above mentioned, P and PC dispersions with a content in Pluronic® equals to 10 mM (either loaded or not loaded with resveratrol) showed the most adequate sol–gel transition temperature, allowing their easy administration as a low viscosity liquid and rapidly transforming into gels at the temperature of the ocular surface (35 °C).

3.6. HET-CAM assay and FET test using the zebrafish model

Resveratrol has shown ocular safety when instilled in a rabbit model (Draize test) encapsulated in Soluplus® micelles at concentration as high as 5 mg/mL. Chronic toxicity tests, carried out using human corneal epithelial cells (HCECs) cultures at lower concentrations, revealed cytocompatibility up to 0.5 mg of resveratrol per mL (Li et al., 2020). The search for alternatives to the Draize test have pointed out the Hen's Egg Test on the Chorioallantoic Membrane (HET-CAM) assay and the zebrafish embryo toxicity test (FET) as preferable methods that fulfil 3Ŕs principles. The HET-CAM assay and the FET test are not considered an

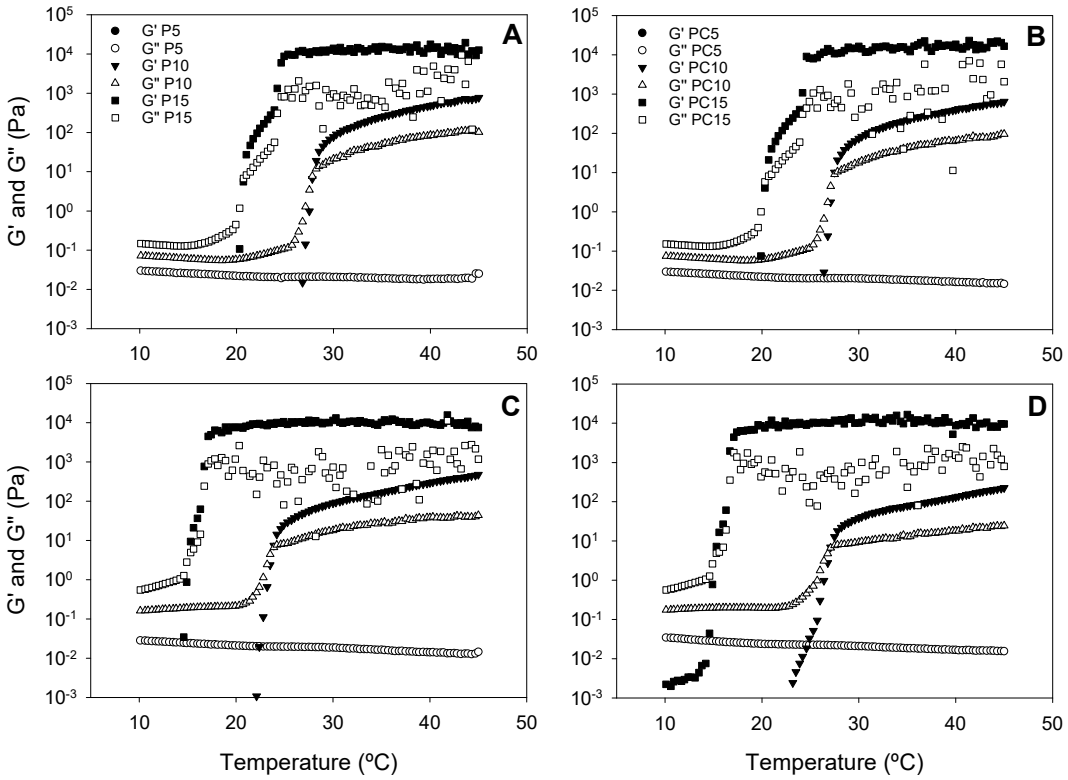

Fig. 3. Rheological behavior of Pluronic® F127 (A, C) and Pluronic®/casein (B, D) dispersions non-loaded (A, B) and loaded with resveratrol (C, D) in phosphate buffer pH 7 as a function of temperature.

animal procedure. The chick chorioallantoic membrane is not innervated, and the Institutional Animal Care and Use Committee (IACUC) and the USA National Institutes of Health established that a chick embryo does not experience pain until embryonal day (ED) 14 and is not considered as a living animal until ED17 (Ribatti, 2016; Kundeková et al., 2021). According to the European Directive 2010/63/EU, the zebrafish embryos until the onset of independent feeding at 120 h post fertilization (hpf) are exempt from legal obligations regarding the protection of animals used for scientific purposes (EuropeanUnion, 2010).

The HET-CAM assay allows evaluating, in a fast and sensitive way, the potential ocular irritancy of the formulations by monitoring changes in the CAM of fertilized eggs, which serves as an analog of the conjunctiva (ICCVAM, 2010). Thus, the potential acute ocular irritation of the prepared formulations was monitored for 5 min in terms of hemorrhage, vascular lysis and coagulation. None of these events was observed for the resveratrol-loaded micelles neither for the non-loaded counterparts when directly applied to the CAM (**Figure S8**). The irritation score (IS) for the negative control and the tested formulations was 0.00. Differently, the IS registered for the positive control (NaOH 0.1 N) was 19.59. These findings mean that the micelle components (Pluronic® F127 and casein) at the concentrations tested as well as the exposition to remarkably high doses of resveratrol are not expected to trigger ocular irritation.

The FET test using zebrafish embryos is being pointed out as suitable for predicting both biocompatibility and ecotoxicity of nanomaterials and pharmaceutical excipients used to develop drug nanocarriers (Hering et al., 2020). Moreover, many human diseases, including relevant ocular pathologies, can be reproduced in zebrafish embryos, which allows screening new treatments in terms of safety and efficacy in a much faster and cheaper way than using mammalian models and avoiding ethics concerns (Zhang et al., 2018; Lee and Yang, 2021; Hernández-Núñez et al., 2022). Although the FET tests carried out with polymeric micelles are still limited, a previous report revealed a 50 % lethal concentration (LC_{50}) of 5.21 % for Pluronic® F127 at 72 hpf (Hering et al., 2020). Therefore, single and mixed micelles prepared with 5, 10 and 15 mM (i.e., 6.3, 12.6 and 18.9 %) Pluronic® F127, both blank and loaded with resveratrol (0.4 mg/mL), were suitably diluted (20-times) in the growing medium up to a final concentration of 0.02 mg resveratrol per mL. It should be noted that, when intended for ophthalmic purposes, few minutes after ocular instillation, the concentration on the eye surface of the formulation components (both drug and excipients) rapidly declines. Thus, the zebrafish embryo toxicity tests were carried out in the range of concentrations expected to be achieved in the anterior segment tissues if the drug would get access to them (Lee and Yang, 2021).

Survival percentage plots are shown in Fig. 4. No formulation reached the LC_{50}, but single and mixed micelles prepared with 15 mM Pluronic® F127 caused approx. 30 % mortality in the 48–96 h. The percentages of survival increased as the content in Pluronic® F127 decreased, especially for formulations loaded with resveratrol and that did not contain casein (Fig. 4 **A**). In the case of mixed micelles, the presence of resveratrol did not cause relevant changes in the survival percentage (Fig. 4 **B**). Overall, these values indicated that resveratrol-loaded Pluronic® F127 (5 and 10 mM) single micelles are biocompatible, while the presence of casein may induce some deleterious effects on long-term viability that are not attenuated by the presence of resveratrol. Although casein hydrolysates (at 0.04 %) have been proved to be safe in a larvae model (Carrillo et al., 2017), casein was demonstrated to interfere with the lipid metabolism, inducing a decrease in body size and reduction of fat mass in male and female zebrafish (Smith et al., 2013). These effects might be behind the enhanced mortality of embryos observed for the resveratrol-loaded mixed micelles, but this issue requires further assessment.

3.7. Antioxidant properties

The DPPH assay was carried out to elucidate the feasibility of the developed single and mixed micelles to load and release resveratrol

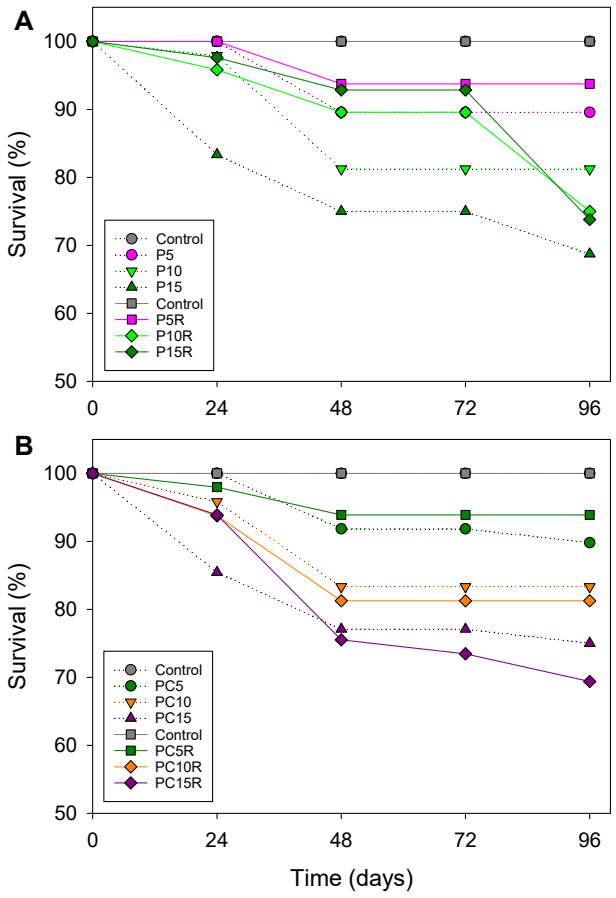

Fig. 4. Survival of *Danio rerio* embryos as observed under presence of the tested single (A) and mixed (B) micelles formulations (final concentration diluted 1/20).

without compromising its antioxidant activity. The possible antioxidant capacity of blank micelles and the phosphate buffer pH 7 used to prepare all formulations was also evaluated to confirm that there were no leaching substances that could cause artifacts during the test. The DPPH scavenging capacity was expressed as μg/mL in the reaction medium and as percentage as previously described (Vivero-Lopez et al., 2021a). The changes in color of the tested formulations after the DPPH assay clearly evidenced the strong antioxidant activity of resveratrol encapsulated in the micelles, which turned the medium yellow, compared to the purple color of non-antioxidant non-loaded micelles (**Figures S9 and S10**).

According to the results (Table 3), the scavenging effect registered for resveratrol-loaded micelles was higher as the content in Pluronic® F127 increased, especially in the mixed micelles, which was in good agreement with the higher content in resveratrol (Table 2). The antioxidant capacity of the phosphate buffer pH 7 was significantly lower ($p < 0.05$) than that of the micelles. No statistically differences were registered between the phosphate buffer pH 7 and the non-loaded micelles. These results confirmed that resveratrol can be incorporated and released from all formulations while preserving its antioxidant capacity. Indeed, even for the resveratrol encapsulated in the single and mixed micelles prepared with 5 mM Pluronic® F127 (P5 and PC5) the antioxidant effect was remarkably high.

Table 3
DPPH levels (μg/mL) and DPPH scavenging effect (%). All data are mean ± standard deviation (n = 3).

Formulation	DPPH (μg/mL)	Scavenging effect (%)
P2.5R	9.8 ± 0.3	20.3 ± 2.2
P5R	9.3 ± 0.1	27.7 ± 1.1
P7.5R	9.4 ± 0.0	27.5 ± 0.3
P10R	9.6 ± 0.2	26.6 ± 1.6
P15R	8.6 ± 0.6	34.6 ± 4.6
PC2.5R	9.4 ± 0.8	28.0 ± 5.9
PC5R	8.1 ± 0.1	38.0 ± 0.9
PC7.5R	8.5 ± 0.1	35.0 ± 1.1
PC10R	8.1 ± 0.7	38.9 ± 5.3
PC15R	6.8 ± 0.5	44.3 ± 4.4
PBS	12.4 ± 0.3	4.8 ± 2.0

3.8. Ability to inhibit bacterial growth

Contamination of multidose eyedrops is one of the main causes of ocular infections worldwide (Teuchner et al., 2015, Kyei et al., 2019). The addition of preservatives may prevent severe infections but may cause allergic or inflammatory reactions in long term use (Baudouin et al., 2010). Thus, the development of topical ophthalmic formulations with capacity to inhibit bacterial growth may avoid the use of preservatives and their associated adverse effects. In this regard, resveratrol may play a role as biofilm inhibitor (Vestergaard and Ingmer, 2019) and as prebiotic, restoring ocular microbiota (Petrillo et al., 2020).

The capacity of all formulations to inhibit bacterial growth was challenged against *S. aureus* and *P. aeruginosa,* two opportunistic bacteria that are involved in microbial keratitis (Bispo et al., 2015). First, resveratrol itself was tested at various concentrations (10–300 μg/mL) in ethanol:water 50:50 v/v. Higher concentrations of resveratrol in ethanol:water 50:50 v/v were not studied due to poor aqueous solubility of the compound and to avoid a high concentration of ethanol in the medium. In all cases, the concentration of ethanol remained at 5 % in the bacterial growth medium. Thus, the growth of bacteria inoculum in the presence of 5 % ethanol was also investigated.

Medium containing 5 % ethanol slowed down the growth of both bacteria (Fig. 5 **A** and **B**) but did not affect the optical density obtained at

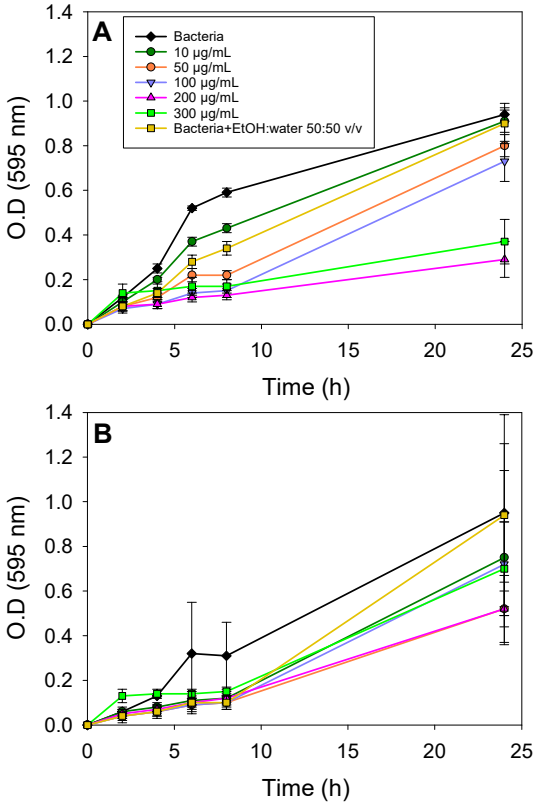

Fig. 5. Growth of *Staphylococcus aureus* (A) and *Pseudomonas aeruginosa* (B) in media containing different concentrations of resveratrol.

24 h, which was similar for both bacteria (0.90 ± 0.09 for *S. aureus*, and 0.94 ± 0.45 for *P. aeruginosa*). A resveratrol concentration of 10 μg/mL did not affect and even increased the growth of *S. aureus* compared to the presence of ethanol in the medium. The growth of *S. aureus* was slowed down when the resveratrol concentration was equal to or higher than 50 μg/mL **(**Fig. 5 **A)**. Strong inhibitory concentrations were found for 200 and 300 μg resveratrol per mL. In the case of *P. aeruginosa,* a decrease in its growth was observed after 8 h of incubation **(**Fig. 5 **B)**. The optical density registered at 24 h decreased with the increase in resveratrol concentration.

Then, the capacity of single and mixed micelles, loaded and not with resveratrol, to inhibit the growth of both bacteria was studied. Bacteria inoculum diluted with PBS was used as control for comparative purposes. In the case of *S. aureus*, a decrease in its growth was observed for resveratrol-loaded single micelles prepared with 10 mM (P10R) and 15 mM (P15R) Pluronic® **(**Fig. 6 **A**; codes 2 and 3 in Table 4**)**, something expected considering the higher amount of resveratrol encapsulated by these formulations. Also, blank micelles prepared with these same concentrations caused a statistically significant decrease in the growth of the bacteria at 6 and 8 h (codes 5 and 6 in Table 4**)**. For mixed micelles, once again P10R and P15R led to statistically significant decreases in bacteria growth at 4, 6 and 8 h **(**Fig. 6 **B).** The decrease was also significant for PC15R at 24 h, and for blank micelles at 6 and 8 h (Table 4).

The growth of *P. aeruginosa* is shown in Fig. 6 **C and D**. The initial turbidity in *P. aeruginosa* growing media may be caused by both the formulations and the biofilm. Both blank and resveratrol-loaded single micelles reduced the growth at 6 h and 8 h, while mixed micelles only caused a decrease at 8 h (Table 5). No differences were shown between resveratrol-loaded and non-loaded micelles, which suggests that the decrease in the growth may be related to a direct effect of Pluronic® F127. This finding is in good agreement with a recent report on the effect of Pluronic® F127 dispersions (0.79 mM) on *Pseudomonas* spp. and *Klebsiella* spp. biofilms, showing a strong inhibitory activity (Eid et al., 2020), although the mechanisms are still to be elucidated.

3.9. *Ex vivo corneal and scleral permeability tests*

Polymeric micelles constitute excellent nanocarriers to improve the solubility and tissue permeability of hydrophobic compounds like resveratrol (Grimaudo et al., 2019, Mandal et al., 2017; Durgun et al., 2020). Since P15R and PC15R showed limited biocompatibility in the FET model, they were discarded for further studies. The capacity of resveratrol formulated in P10R and PC10R micelles to permeate through porcine cornea and sclera together with its capacity to remain in these tissues was evaluated through an *ex vivo* permeability test. The test was carried out using porcine tissues given their close similarity to the human eye (Alambiaga-Caravaca et al., 2020). In cornea **(**Fig. 7**A)**, no quantifiable amounts of resveratrol were recorded in the receptor chamber in the first 3 h. No differences were observed for the permeability through cornea between single and mixed micelles.

Differently, resveratrol showed an increased permeability through sclera (Fig. 7**B)** recording quantifiable amounts from the first hour of experiment. Single micelles loaded with resveratrol led to an increase in scleral permeability **(**Fig. 7**B).** Both single and mixed micelles improved notably the permeability of resveratrol through both tissues compared to previously developed HEMA- and silicone-based hydrogels loaded with resveratrol and a less concentrated resveratrol solution (70 μg/mL), which did not provide measurable amounts of resveratrol to the receptor chamber (Vivero-Lopez et al., 2021a). It should be noted that P10R and PC10R micelles solubilized nearly 9 mg of resveratrol per mL. The enhanced permeation correlated well with other reports where the capacity of micellar systems composed of Soluplus® to increase the permeability of different drugs as acyclovir or α-lipoic acid was demonstrated (Alvarez-Rivera et al., 2016, Varela-Garcia et al., 2018).

The steady state flux (J) and the apparent permeability coefficient

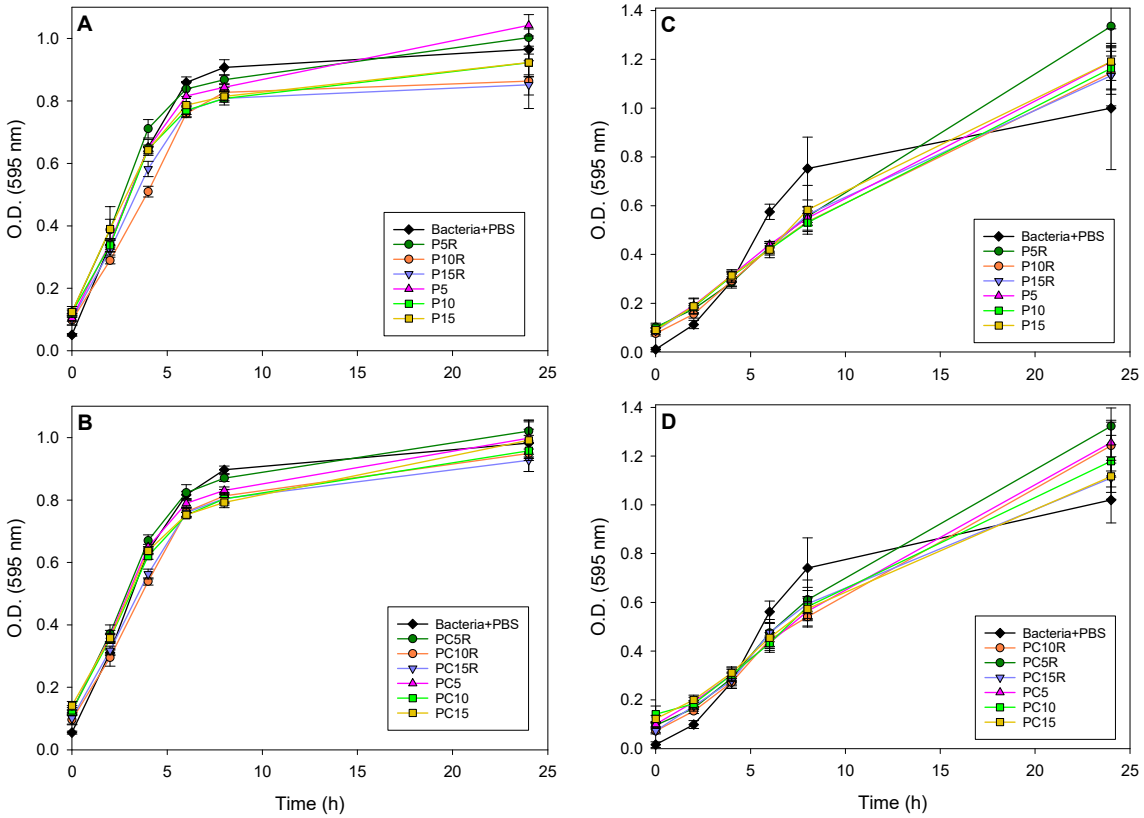

Fig. 6. Bacterial growth of *Staphylococcus aureus* (A and B) and *Pseudomonas aeruginosa* (C and D) in the presence of different single (A, C) and mixed micelles (B, D).

Table 4
Statistical analysis (ANOVA and multiple range test) of the optical density values recorded for *S. aureus* growth in the presence of P5R (1), P10R (2), P15R (3), P5 (4), P10 (5), P15 (6), and the bacteria inoculum diluted with PBS (7, control) (n = 6). Data in Fig. 6 A and B. In the multiple range test column, the values are ranked in increasing order. The code (7) of the bacteria growing in the absence of the formulations is highlighted in red.

Formulation	Time (h)	$F_{6,35}$	*p*	Multiple range test
Single micelle	4	63.15	0.000	2 3 6 5 4 7 1
	6	17.10	0.000	2 3 5 6 4 1 7
	8	28.15	0.000	5 3 6 2 4 1 7
	24	12.88	0.000	3 2 5 6 7 1 4
Mixed micelle	4	83.47	0.000	2 3 5 7 6 4 1
	6	26.93	0.000	5 6 3 2 4 7 1
	8	37.49	0.000	6 5 3 2 4 1 7
	24	2.82	0.024	3 2 5 7 6 4 1

Table 5
Statistical analysis (ANOVA and multiple range test) of the optical density values recorded for *P. aeruginosa* growth in the presence of P5R (1), P10R (2), P15R (3), P5 (4), P10 (5), P15 (6), and the bacteria inoculum diluted with PBS (7, control) (n = 6). Data in Fig. 6 C and D. In the multiple range test column, the values are ranked in increasing order. The code (7) of the bacteria growing in the absence of the formulations is highlighted in red.

Formulation	Time (h)	$F_{6,35}$	*p*	Multiple range test
Single micelle	4	2.35	0.052	No significant differences
	6	34.43	0.000	6 5 3 2 1 4 7
	8	7.74	0.000	5 2 4 1 3 6 7
	24	3.31	0.011	7 3 2 5 4 6 1
Mixed micelle	4	2.53	0.038	2 7 3 1 4 5 6
	6	0.85	0.658	No significant differences
	8	5.07	0.001	2 4 6 5 3 1 7
	24	8.13	0.000	7 3 6 5 2 4 1

(P_{app}) of resveratrol in both corneal and scleral tissues are shown in Table 6. For the calculations, there was no significant change in concentration in the donor chamber over time, and values of approx. 9 mg/mL were maintained after 6 h. Also, resveratrol stability in the PPG: water 40:60 v/v medium at 37 °C was previously tested for a known concentration of resveratrol (5 μg/mL) and the HPLC chromatograms of the solutions at time 0 h and after 6 h at 37 °C were superimposable. The obtained permeability coefficients were lower than those previously reported for other drugs like α-lipoic acid, aciclovir or *trans*-ferulic acid (Alvarez-Rivera et al., 2016; Varela-Garcia et al., 2018; Varela-Garcia et al., 2020); the steady state flux values were in good agreement with the values reported for aciclovir in Soluplus® micelles but resveratrol concentration in the micelles was 7.5 times larger. Relevantly, mixed micelles provided much lower resveratrol permeability through sclera (Fig. 7**B**, Table 6), although tissue accumulation was found to be similar. Resveratrol accumulation in sclera for single (475.91 ± 219.99 μg/cm^2) and mixed (467.59 ± 20.51 μg/cm^2) micelles was not statistically significant, and it was much higher than in cornea for single (83.59 ± 19.45 μg/cm^2) and mixed (62.58 ± 6.85 μg/cm^2) micelles. As expected from the greater permeability of sclera tissue compared to cornea, single

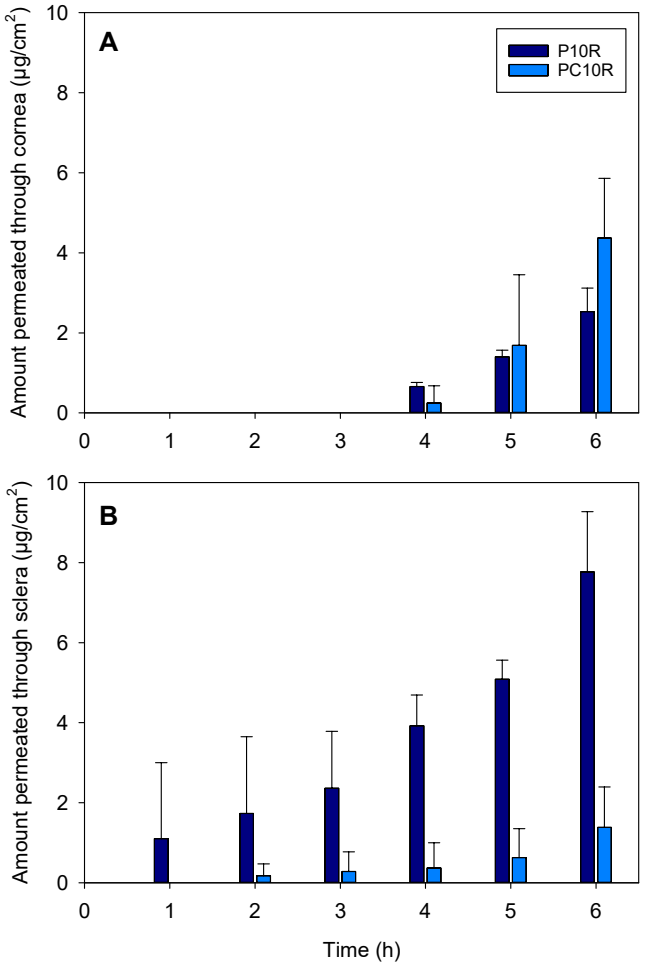

Fig. 7. Amounts of resveratrol permeated trough cornea (A) and sclera (B) when released from P10R and PC10R micelles (9 mg resveratrol/mL) (n = 3; mean values and standard deviations).

Table 6
The lag time (t_{lag}), steady state flux (J) and apparent permeability coefficient (P_{app}) of resveratrol released from P10R and PC10R dispersions for cornea and sclera tissues (n = 3; mean value ± standard deviation).

Formulation	Cornea			Sclera		
	t_{lag} (h)	J (µg/cm²h)	P_{app} (cm/s)	t_{lag} (h)	J (µg/cm²h)	P_{app} (cm/s)
P10R	3.0 ± 0.1	0.94 ± 0.25	$2.51 \times 10^{-8} \pm 0.60 \times 10^{-8}$	0.0 ± 0.1	1.57 ± 0.65	$4.69 \times 10^{-8} \pm 1.92 \times 10^{-8}$
PC10R	4.0 ± 0.1	2.06 ± 0.95	$5.13 \times 10^{-8} \pm 2.53 \times 10^{-8}$	1.0 ± 0.1	0.28 ± 0.17	$0.75 \times 10^{-8} \pm 0.45 \times 10^{-8}$

(Pluronic® F127) micelles passed more easily through the sclera and delivered more resveratrol to the receptor medium (Gaudana et al., 2010). The poor permeability recorded for mixed micelles suggested specific interactions of casein with the sclera tissue, which might be favored by its less compact structure compared to cornea (Crespo-Villanueva et al., 2018).

3.10. Mucoadhesion tests

P10R and PC10R formulations were further investigated regarding their mucoadhesion properties. Since variability among tissues from different animals can be expected, each cornea and sclera piece was tested against the formulation and also against the control PBS medium alternatively, five times for each medium. Two independent experiments were carried out for each tissue and formulation. Detachment force and mucoadhesion work values are shown in Table S3. In the case of cornea, the values recorded for P10R and PC10R formulations were significantly larger than for control PBS medium (ANOVA; $p < 0.05$). The results obtained for sclera evidenced that although the mean values of detachment force and mucoadhesion work were in all cases larger for P10R and PC10R formulations, the differences with the control were minor, probably due to the large standard deviations recorded. Overall, the mucoadhesion tests indicate that the formulations may remain longer on the cornea surface than the vehicle without micelles.

3.11. In vivo experiments

Since biocompatibility and permeability concerns arose for the mixed micelles, *in vivo* studies in rabbits were only carried out for the P10R formulation, which was positioned as the most suitable for resveratrol delivery to the eyes. Resveratrol levels in tear fluid were monitored for 8 h after one drop instillation (50 µL; 4 mg resveratrol per mL) in the right eye (Fig. 8**A;** raw data available in **Table S4**). The experiments were carried out in quadruplicate and the left eyes served as controls. Measurable levels of resveratrol were detected in tear fluid for 8 h, although the concentration rapidly decreased in the first two hours. Relevantly, high levels of resveratrol were detected in cornea, sclera and retina (Fig. 8**B**) of right eyes 8 h after the eye drop instillation (raw data available in **Table S5**). Resveratrol was not detected in the left eyes (controls). Importantly, the slit lamp images (Fig. 8**C**) confirmed the good ocular tolerance of the developed formulation. These findings pointed out the capability of the micelles to efficiently supply resveratrol to anterior and posterior segments of the eye, which agrees with recent reports on ocular delivery using other drug-loaded micelles (Durgun et al., 2020).

Although ocular biodistribution of resveratrol was not reported in previous studies, Li et al. (2020) observed that Soluplus® micelles solution of a similar resveratrol concentration (5 mg/mL) favored resveratrol accumulation in mice cornea and decreased pro-inflammatory cytokines in the first hours after repeated instillations. Our data evidenced that even 8 h after one drop instillation of the P10R formulation, resveratrol levels were still significantly high in ocular tissues, particularly in cornea, which may open novel alternatives for the prophylaxis and treatment of oxidation- or inflammation-related ocular diseases.

4. Conclusions

Single and mixed micelles composed of Pluronic® F127 and Pluronic® F127/casein evidenced an excellent capability to encapsulate resveratrol enhancing the apparent solubility>50 times and preserving the antioxidant capacity. All formulations also showed remarkable physical stability after dilution and during prolonged storage at 4 °C protected from light and facilitated resveratrol penetration through cornea and sclera *ex vivo*. Compared to single Pluronic® F127 micelles, mixed micelles had similar sizes, but the presence of casein endowed the micelles with more negative Zeta-potential and slightly increased resveratrol solubility and its antioxidant activity, while also exhibiting sol-to-gel transitions in an adequate temperature range. These features might be favorable for ocular administration, but the slightly higher toxicity found in FET tests for formulations combining casein and resveratrol demands further assessment of the safety of Pluronic® F127/casein mixed micelles. Pluronic® F127 10 mM single micelles are

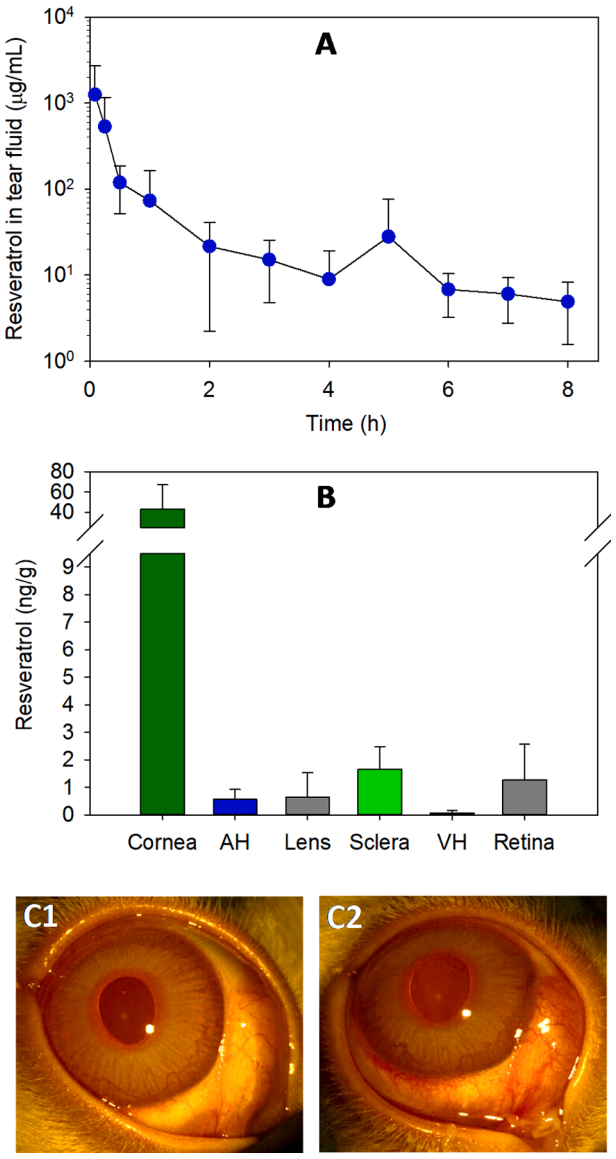

Fig. 8. (A) Resveratrol levels in tear fluid after one drop (50 μL) instillation of P10R micelles in the right eye of male New Zealand white rabbits (n = 4); (B) resveratrol levels in eye tissues 8 h after the eye drop instillation; and (C1, C2) slit lamp images before (C1; t = 0 h) and after (C2; t = 8 h) the administration of P10R eye drops.

pointed out as adequate formulations for ocular delivery of resveratrol since they combine remarkably high capability to solubilize resveratrol and to preserve its antioxidant properties, to hinder biofilm development, to form gels in an adequate temperature window, and to favor resveratrol permeability through corneal and scleral tissues.

CRediT authorship contribution statement

Maria Vivero-Lopez: Conceptualization, Data curation, Writing – original draft, Writing – review & editing. **Chiara Sparacino:** Data curation, Writing – original draft. **Ana Quelle-Regaldie:** Data curation, Writing – original draft. **Laura Sánchez:** Conceptualization, Writing – review & editing. **Eva Candal:** Conceptualization, Writing – review & editing. **Antón Barreiro-Iglesias:** Conceptualization, Writing – review & editing. **Fernando Huete-Toral:** Conceptualization, Writing – review & editing. **Gonzalo Carracedo:** Conceptualization, Writing – review & editing. **Ana Otero:** Conceptualization, Writing – review & editing. **Angel Concheiro:** Conceptualization, Supervision, Writing – review & editing. **Carmen Alvarez-Lorenzo:** Conceptualization, Supervision, Data curation, Writing – original draft, Writing – review & editing.

Declaration of Competing Interest

The authors declare that they have no known competing financial interests or personal relationships that could have appeared to influence the work reported in this paper.

Data availability

Data will be made available on request.

Acknowledgements

The authors are grateful to Mabel Loza and Cristina Val García from BioFarma Research Group (CiMUS) for their help with UPLC experiments, and to Ana F. Pereira-da-Mota (USC) for help with *in vivo* experiments.

Funding: The work was supported by MCIN/AEI/10.13039/501100011033 [PID 2020-113881RB-I00 to A.C. and C.A.-L., and PID2020-115121GB-I00 to L.S. and A.B.-I.], Spain, Xunta de Galicia [ED431C 2020/17], and FEDER. M. Vivero-Lopez acknowledges Xunta de Galicia (Consellería de Cultura, Educación e Ordenación Universitaria) for a predoctoral research fellowship [ED481A-2019/120].

Appendix A. Supplementary material

Supplementary data to this article can be found online at https://doi.org/10.1016/j.ijpharm.2022.122281.

References

Alambiaga-Caravaca, A.M., Calatayud-Pascual, M.A., Rodilla, V., Concheiro, A., López-Castellano, A., Alvarez-Lorenzo, C., 2020. Micelles of progesterone for topical eye administration: Interspecies and intertissues differences in ex vivo ocular permeability. Pharmaceutics 12 (8), 702.

Al Khateb, K., Ozhmukhametova, E.K., Mussin, M.N., Seilkhanov, S.K., Rakhypbekov, T. K., Lau, W.M., Khutoryanskiy, V.V., 2016. In situ gelling systems based on Pluronic F127/Pluronic F68 formulations for ocular drug delivery. Int. J. Pharm. 502 (1–2), 70–79.

Alvarez-Rivera, F., Fernández-Villanueva, D., Concheiro, A., Alvarez-Lorenzo, C., 2016. α-Lipoic acid in Soluplus® polymeric nanomicelles for ocular treatment of diabetes-associated corneal diseases. J. Pharm. Sci. 105 (9), 2855–2863.

Alvarez-Rivera, F., Serro, A.P., Silva, D., Concheiro, A., Alvarez-Lorenzo, C., 2019. Hydrogels for diabetic eyes: Naltrexone loading, release profiles and cornea penetration. Mater. Sci. Eng., C 105, 110092.

Amri, A., Chaumeil, J.C., Sfar, S., Charrueau, C., 2012. Administration of resveratrol: what formulation solutions to bioavailability limitations? J. Control. Release 158 (2), 182–193.

Bachar, M., Mandelbaum, A., Portnaya, I., Perlstein, H., Even-Chen, S., Barenholz, Y., Danino, D., 2012. Development and characterization of a novel drug nanocarrier for oral delivery, based on self-assembled β-casein micelles. J. Control. Release 160 (2), 164–171.

Baudouin, C., Labbé, A., Liang, H., Pauly, A., Brignole-Baudouin, F., 2010. Preservatives in eyedrops: the good, the bad and the ugly. Prog. Retinal Eye Res. 29 (4), 312–334.

Behl, T., Kaur, I., Kotwani, A., 2016. Implication of oxidative stress in progression of diabetic retinopathy. Surv. Ophthalmol. 61 (2), 187–196.

Bispo, P.J., Haas, W., Gilmore, M.S., 2015. Biofilms in infections of the eye. Pathogens 4 (1), 111–136.

Bola, C., Bartlett, H., Eperjesi, F., 2014. Resveratrol and the eye: activity and molecular mechanisms. Graefe's Arch. Clin. Exp. Ophthalmol. 252 (5), 699–713.

Bourassa, P., Bariyanga, J., Tajmir-Riahi, H.A., 2013. Binding sites of resveratrol, genistein, and curcumin with milk α-and β-caseins. J. Phys. Chem. B 117 (5), 1287–1295.

Cabrera-Pérez, M.A., Bermejo-Sanz, M., Mangas Sanjuan, V. (2015). Importance and applications of cell- and tissue-based in vitro models for drug permeability screening. In: Concepts and Models for Drug Permeability Studies (Sarmento, B., Ed.), Elsevier, pp. 3-29. DOI: 10.1016/B978-0-08-100094-6.00002-X.

Cadena, P.G., Pereira, M.A., Cordeiro, R.B.S., Cavalcanti, I.M.F., Barros Neto, B., Pimentel, M.d.C.C.B., Lima Filho, J.L., Silva, V.L., Santos-Magalhães, N.S., 2013. Nanoencapsulation of quercetin and resveratrol into elastic liposomes. Biochimica et Biophysica Acta (BBA)-Biomembranes 1828 (2), 309–316.

Calderon, G.D., Juarez, O.H., Hernandez, G.E., Punzo, S.M., De la Cruz, Z.D., 2017. Oxidative stress and diabetic retinopathy: development and treatment. Eye 31 (8), 1122–1130.

Carrillo, W., Guzmán, X., Vilcacundo, E., 2017. Native and heated hydrolysates of milk proteins and their capacity to inhibit lipid peroxidation in the zebrafish larvae model. Foods 6 (9), 81.

Cejka, C., & Cejkova, J. (2015). Oxidative stress to the cornea, changes in corneal optical properties, and advances in treatment of corneal oxidative injuries. *Oxid. Med. Cellu. Long., 2015,* 591530.

Chen, Y., Meng, J., Li, H., Wei, H., Bi, F., Liu, S., Tang, K., Guo, H., Liu, W., 2019. Resveratrol exhibits an effect on attenuating retina inflammatory condition and damage of diabetic retinopathy via PON1. Exp. Eye Res. 181, 356–366.

Crespo-Villanueva, A., Gumí-Audenis, B., Sanz, F., Artzner, F., Mériadec, C., Rousseau, F., Lopez, C., Giannotti, M.I., Guyomarc'h, F., 2018. Casein interaction with lipid membranes: Are the phase state or charge density of the phospholipids affecting protein adsorption? Biochimica et Biophysica Acta (BBA) - Biomembranes 1860 (12), 2588–2598.

Dammak, A., Huete-Toral, F., Carpena-Torres, C., Martin, A., Pastrana, C., Carracedo, G., 2021. From oxidative stress to inflammation in the posterior ocular diseases: diagnosis and treatment. Pharmaceutics 13 (9), 1376.

Del Regno, A., Warren, P.B., Bray, D.J., Anderson, R.L., 2021. Critical micelle concentrations in surfactant mixtures and blends by simulation. J. Phys. Chem. B 125 (22), 5983–5990.

Delmas, D., Cornebise, C., Courtaut, F., Xiao, J., Aires, V., 2021. New highlights of resveratrol: A review of properties against ocular diseases. Int. J. Mol. Sci. 22 (3), 1295.

Di Donato, C., Iacovino, R., Isernia, C., Malgieri, G., Varela-Garcia, A., Concheiro, A., Alvarez-Lorenzo, C., 2020. Polypseudorotaxanes of Pluronic® F127 with combinations of α-and β-cyclodextrins for topical formulation of acyclovir. Nanomaterials 10 (4), 613.

Dinte, E., Vostinaru, O., Samoila, O., Sevastre, B., Bodoki, E., 2020. Ophthalmic nanosystems with antioxidants for the prevention and treatment of eye diseases. Coatings 10 (1), 36.

Dogru, M., Kojima, T., Simsek, C., & Tsubota, K. (2018). Potential role of oxidative stress in ocular surface inflammation and dry eye disease. *Invest. Ophthalmol. Vis. Sci.*, *59* (14), DES163-DES168.

Durgun, M.E., Güngör, S., Özsoy, Y., 2020. Micelles: Promising ocular drug carriers for anterior and posterior segment diseases. J. Ocul. Pharmacol. Ther. 36 (6), 323–341.

Eid, D., Sayed, O.M., Hozayen, W.G., Azmy, A.F., 2020. Battling biofilm forming nosocomial pathogens using chitosan and Pluronic F127. J. Pure Appl. Microbiol. 14 (3), 1893–1903.

EMA. https://www.ema.europa.eu/en/search/search?search_api_views_fulltext=poloxamer+AND+ocular ; accessed January 2022.

European Union, 2010. Directive 2010/63/EU of the European Parliament and of the Council of 22 September 2010 on the protection of animals used for scientific purposes. accessed January 2022. https://eur-lex.europa.eu/legal-content/EN/TXT/HTML/?uri=CELEX:32010L0063&from=EN;.

Gandhi, S., Roy, I., 2019. Doxorubicin-loaded casein nanoparticles for drug delivery: Preparation, characterization and in vitro evaluation. Int. J. Biol. Macromol. 121, 6–12.

Gaudana, R., Ananthula, H.K., Parenky, A., Mitra, A.K., 2010. Ocular drug delivery. AAPS J. 12 (3), 348–360.

Ghadiri Soufi, F., Arbabi-Aval, E., Rezaei Kanavi, M., Ahmadieh, H., 2015. Anti-inflammatory properties of resveratrol in the retinas of type 2 diabetic rats. Clin. Exp. Pharmacol. Physiol. 42 (1), 63–68.

Glab, T.K., Boratyński, J., 2017. Potential of casein as a carrier for biologically active agents. Top. Curr. Chem. 375 (4), 1–20.

Grimaudo, M.A., Pescina, S., Padula, C., Santi, P., Concheiro, A., Alvarez-Lorenzo, C., Nicoli, S., 2019. Topical application of polymeric nanomicelles in ophthalmology: A review on research efforts for the noninvasive delivery of ocular therapeutics. Expert Opin. Drug Del. 16 (4), 397–413.

Hering, I., Eilebrecht, E., Parnham, M.J., Günday-Türeli, N., Türeli, A.E., Weiler, M., Schäfers, C., Fenske, M., Wacker, M.G., 2020. Evaluation of potential environmental toxicity of polymeric nanomaterials and surfactants. Environ. Toxicol. Pharmacol. 76, 103353.

Hernández-Núñez, I., Vivero-Lopez, M., Quelle-Regaldie, A., DeGrip, W.J., Sánchez, L., Concheiro, A., Alvarez-Lorenzo, C., Candal, E., Barreiro-Iglesias, A., 2022. Embryonic nutritional hyperglycemia decreases cell proliferation in the zebrafish retina. Histochem. Cell Biol. 158 (4), 401–409.

Huang, D.-D., Shi, G., Jiang, Y., Yao, C., Zhu, C., 2020. A review on the potential of Resveratrol in prevention and therapy of diabetes and diabetic complications. Biomed. Pharmacother. 125, 109767.

ICCVAM. *ICCVAM Test Method Evaluation Report: Current Validation Status of In Vitro Test Methods Proposed for Identifying Eye Injury Hazard Potential of Chemicals and Products*; NIH Publication No. 10-7553; Research Triangle Park, National Institute of Environmental Health Sciences: Durham, NC, USA, 2010; p. 1324.

Jadhav, P., Bothiraja, C., Pawar, A., 2016. Resveratrol-piperine loaded mixed micelles: formulation, characterization, bioavailability, safety and in vitro anticancer activity. RSC Adv. 6 (114), 112795–112805.

Kang, Q., Yang, C., 2020. Oxidative stress and diabetic retinopathy: Molecular mechanisms, pathogenetic role and therapeutic implications. Redox Biol. 37, 101799.

Katekar, R., Thombre, G., Riyazuddin, M., Husain, A., Rani, H., Praveena, K.S., Gayen, J. R., 2020. Pharmacokinetics and brain targeting of trans-resveratrol loaded mixed micelles in rats following intravenous administration. Pharm. Dev. Technol. 25 (3), 300–307.

Kessler, A., Menéndez-Aguirre, O., Hinrichs, J., Stubenrauch, C., Weiss, J., 2014. αs-Casein—PE6400 mixtures: Surface properties, miscibility and self-assembly. Colloids Surf., B 118, 49–56.

Kimpel, F., Schmitt, J.J., 2015. Milk proteins as nanocarrier systems for hydrophobic nutraceuticals. J. Food Sci. 80 (11), R2361–R2366.

Kimura, A., Namekata, K., Guo, X., Noro, T., Harada, C., Harada, T., 2017. Targeting oxidative stress for treatment of glaucoma and optic neuritis. Oxid. Med. Cell. Longevity 2017, 1–8.

Kundeková, B., Mácajová, M., Meta, M., Cavarga, I., Bilcík, B., 2021. Chorioallantoic membrane models of various avian species: differences and applications. Biology 10 (4), 301.

Kyei, S., France, D., Asiedu, K., 2019. Microbial contamination of multiple-use bottles of fluorescein ophthalmic solution. Clin. Exp. Optometry 102 (1), 30–34.

Lee, Y., Yang, J., 2021. Development of a zebrafish screening model for diabetic retinopathy induced by hyperglycemia: Reproducibility verification in animal model. Biomed. Pharmacother. 135, 111201.

Li, M., Zhang, L., Li, R., Yan, M., 2020. New resveratrol micelle formulation for ocular delivery: characterization and in vitro/in vivo evaluation. Drug Dev. Ind. Pharm. 46 (12), 1960–1970.

Lorenzo-Veiga, B., Diaz-Rodriguez, P., Alvarez-Lorenzo, C., Loftsson, T., Sigurdsson, H. H., 2020. In vitro and ex vivo evaluation of nepafenac-based cyclodextrin microparticles for treatment of eye inflammation. Nanomaterials 10 (4), 709.

Mandal, A., Bisht, R., Rupenthal, I.D., Mitra, A.S., 2017. Polymeric micelles for ocular drug delivery: From structural frameworks to recent preclinical studies. J. Control. Release 248, 96–116.

Nagai, N., Isaka, T., Deguchi, S., Minami, M., Yamaguchi, M., Otake, H., Okamoto, N., Nakazawa, Y., 2020. In situ gelling systems using pluronic F127 enhance corneal permeability of indomethacin nanocrystals. Int. J. Mol. Sci. 21 (19), 7083.

Nita, M., Grzybowski, A., 2016. The role of the reactive oxygen species and oxidative stress in the pathomechanism of the age-related ocular diseases and other pathologies of the anterior and posterior eye segments in adults. Oxid. Med. Cell. Longevity 2016, 1–23.

OECD (2006). Fish embryo toxicity (FET) test. OECD guideline for testing of Chemicals. https://www.oecd-ilibrary.org/docserver/9789264203709-en.pdf?expires=1642188277&id=id&accname=guest&checksum=C2E677D38844874F436140FE5D30A0C4; accessed January 2022.

Pandian, S., Jeevanesan, V., Ponnusamy, C., Natesan, S., 2017. RES-loaded pegylated CS NPs for efficient ocular delivery. IET Nanobiotechnol. 11 (1), 32–39.

Paulsson, M., Hägerström, H., Edsman, K., 1999. Rheological studies of the gelation of deacetylated gellan gum (Gelrite) in physiological conditions. Eur. J. Pharm. Sci. 9 (1), 99–105.

Peñalva, R., Morales, J., González-Navarro, C.J., Larrañeta, E., Quincoces, G., Peñuelas, I., Irache, J.M., 2018. Increased oral bioavailability of resveratrol by its encapsulation in casein nanoparticles. Int. J. Mol. Sci. 19 (9), 2816.

Petrillo, F., Pignataro, D., Lavano, M.A., Santella, B., Folliero, V., Zannella, C., Astarita, C., Gagliano, C., Franci, G., Avitabile, T., Galdiero, M., 2020. Current evidence on the ocular surface microbiota and related diseases. Microorganisms 8 (7), 1033.

Phadungath, C., 2005. Casein micelle structure: a concise review. Songklanakarin J. Sci. Technol. 27 (1), 201–212.

Pinazo-Duran, M.D., Shoaie-Nia, K., Zanon-Moreno, V., Sanz-Gonzalez, S.M., del Castillo, J.B., Garcia-Medina, J.J., 2018. Strategies to reduce oxidative stress in glaucoma patients. Curr. Neuropharmacol. 16 (7), 903–918.

Portnaya, I., Khalfin, R., Kesselman, E., Ramon, O., Cogan, U., Danino, D., 2011. Mixed micellization between natural and synthetic block copolymers: β-casein and Lutrol F-127. PCCP 13 (8), 3153–3160.

Raj, J., Uppuluri, K.B., 2015. Metformin loaded casein micelles for sustained delivery: formulation, characterization and in-vitro evaluation. Biomed. Pharmacol. J. 8, 1. http://biomedpharmajournal.org/?p=989.

Rangel-Yagui, C.O., Pessoa Jr, A., Tavares, L.C., 2005. Micellar solubilization of drugs. J. Pharmacy Pharmaceutical Sci. 8 (2), 147–163.

Rehan, F., Ahemad, N., Gupta, M., 2019. Casein nanomicelle as an emerging biomaterial–A comprehensive review. Colloids Surf., B 179, 280–292.

Ribatti, D., 2016. The Chick Embryo Chorioallantoic Membrane (CAM). A multifaceted experimental model. Mech. Dev. 141, 70–77.

Ribeiro, A., Sosnik, A., Chiappetta, D.A., Veiga, F., Concheiro, A., Alvarez-Lorenzo, C., 2012. Single and mixed poloxamine micelles as nanocarriers for solubilization and sustained release of ethoxzolamide for topical glaucoma therapy. J. R. Soc. Interface 9 (74), 2059–2069.

Robinson, K., Mock, C., Liang, D., 2015. Pre-formulation studies of resveratrol. Drug Dev. Ind. Pharm. 41 (9), 1464–1469.

Rodriguez-Perez, A.I., Rodriguez-Tenreiro, C., Alvarez-Lorenzo, C., Concheiro, A., Torres-Labandeira, J.J., 2006. Drug solubilization and delivery from cyclodextrin-pluronic aggregates. J. Nanosci. Nanotechnol. 6 (9–10), 3179–3186.

Semeraro, F., Morescalchi, F., Cancarini, A., Russo, A., Rezzola, S., Costagliola, C., 2019. Diabetic retinopathy, a vascular and inflammatory disease: therapeutic implications. Diab. Metab. 45 (6), 517–527.

Shapira, A., Markman, G., Assaraf, Y.G., Livney, Y.D., 2010. β-casein–based nanovehicles for oral delivery of chemotherapeutic drugs: drug-protein interactions and mitoxantrone loading capacity. Nanomed. Nanotechnol. Biol. Med. 6 (4), 547–555.

Sharma, P.K., Bhatia, S.R., 2004. Effect of anti-inflammatories on Pluronic® F127: micellar assembly, gelation and partitioning. Int. J. Pharm. 278 (2), 361–377.

Smith, D.L., Barry, R.J., Powell, M.L., Nagy, T.R., D'Abramo, L.R., Watts, S.A., 2013. Dietary protein source influence on body size and composition in growing zebrafish. Zebrafish 10 (3), 439–446.

Summerlin, N., Soo, E., Thakur, S., Qu, Z., Jambhrunkar, S., Popat, A., 2015. Resveratrol nanoformulations: challenges and opportunities. Int. J. Pharm. 479 (2), 282–290.

Taveira, S.F., Varela-Garcia, A., dos Santos Souza, B., Marreto, R.N., Martin-Pastor, M., Concheiro, A., Alvarez-Lorenzo, C., 2018. Cyclodextrin-based poly (pseudo) rotaxanes for transdermal delivery of carvedilol. Carbohydr. Polym. 200, 278–288.
Teuchner, B., Wagner, J., Bechrakis, N.E., Orth-Höller, D., Nagl, M., 2015. Microbial contamination of glaucoma eyedrops used by patients compared with ocular medications used in the hospital. Medicine 94 (8), e583.
Toro, M.D., Nowomiejska, K., Avitabile, T., Rejdak, R., Tripodi, S., Porta, A., Reibaldi, M., Figus, M., Posarelli, C., Fiedorowicz, M., 2019. Effect of resveratrol on in vitro and in vivo models of diabetic retinophathy: a systematic review. Int. J. Mol. Sci. 20 (14), 3503.
Turovsky, T., Khalfin, R., Kababya, S., Schmidt, A., Barenholz, Y., Danino, D., 2015a. Celecoxib encapsulation in β-casein micelles: structure, interactions, and conformation. Langmuir 31 (26), 7183–7192.
Turovsky, T., Portnaya, I., Kesselman, E., Ionita-Abutbul, I., Dan, N., Danino, D., 2015b. Effect of temperature and loading on the structure of β-casein/ibuprofen assemblies. J. Colloid Interface Sci. 449, 514–521.
Ung, L., Pattamatta, U., Carnt, N., Wilkinson-Berka, J.L., Liew, G., White, A.J., 2017. Oxidative stress and reactive oxygen species: a review of their role in ocular disease. Clin. Sci. 131 (24), 2865–2883.
Varela-Garcia, A., Concheiro, A., Alvarez-Lorenzo, C., 2020. Cytosine-functionalized bioinspired hydrogels for ocular delivery of antioxidant transferulic acid. Biomater. Sci. 8 (4), 1171–1180.
Varela-Garcia, A., Concheiro, A., Alvarez-Lorenzo, C., 2018. Soluplus micelles for acyclovir ocular delivery: Formulation and cornea and sclera permeability. Int. J. Pharm. 552 (1–2), 39–47.
Vestergaard, M., Ingmer, H., 2019. Antibacterial and antifungal properties of resveratrol. Int. J. Antimicrob. Agents 53 (6), 716–723.
Vivero-Lopez, M., Muras, A., Silva, D., Serro, A.P., Otero, A., Concheiro, A., Alvarez-Lorenzo, C., 2021a. Resveratrol-loaded hydrogel contact lenses with antioxidant and antibiofilm performance. Pharmaceutics 13 (4), 532.
Vivero-Lopez, M., Xu, X., Muras, A., Otero, A., Concheiro, A., Gaisford, S., Basit, A.W., Alvarez-Lorenzo, C., Goyanes, A., 2021b. Anti-biofilm multi drug-loaded 3D printed hearing aids. Mater. Sci. Eng., C 119, 111606.
Zhang, L., Maddison, L.A., Chen, W., 2018. Zebrafish as a model for obesity and diabetes. Front. Cell Dev. Biol. 6, 91.